INSTITUTO POLITÉCNICO DE LISBOA

ESCOLA SUPERIOR DE TECNOLOGIA DA SAÚDE DE LISBOA

IGRT COM CBCT: O IMPACTO NA PRECISÃO EM RADIOTERAPIA

ANA RITA LOPES SIMÕES

ORIENTADORAS:

PROF. MARGARIDA EIRAS, ESCOLA SUPERIOR DE TECNOLOGIA DA SAUDE DE LISBOA

PROF. DOUTORA ISABEL MONTEIRO GRILLO, HOSPITAL DE SANTA MARIA- CHLN

Mestrado em Radiações aplicadas às tecnologias da saúde

Lisboa, 2012

INSTITUTO POLITÉCNICO DE LISBOA
ESCOLA SUPERIOR DE TECNOLOGIA DA SAÚDE DE LISBOA

IGRT COM CBCT: O IMPACTO NA PRECISÃO EM RADIOTERAPIA

ANA RITA LOPES SIMÕES

ORIENTADORAS:
PROF. MARGARIDA EIRAS, ESCOLA SUPERIOR DE TECNOLOGIA DA SAUDE DE LISBOA
PROF. DOUTORA ISABEL MONTEIRO GRILLO, HOSPITAL DE SANTA MARIA- CHLN

JÚRI:
MESTRE MIGUEL PONTES

Mestrado em Radiações aplicadas às tecnologias da saúde

(esta versão incluiu as críticas e sugestões feitas pelo júri)

Lisboa, 2012

IGRT COM CBCT: O IMPACTO NA PRECISÃO EM RADIOTERAPIA

AGRADECIMENTOS

O percurso deste semestre, embora intelectualmente muito estimulante, foi bastante difícil e árduo devido à elevada exigência a que um profissional da área da saúde é submetido no seu dia-a-dia. Assim, é de notar que este percurso, que agora termina, teria sido impossível caso não tivesse contado com a ajuda de muitas pessoas em diferentes momentos e a vários níveis. Assim gostaria de agradecer:

-Às minhas orientadoras, Professora Margarida Eiras e Professora Doutora Isabel Monteiro Grillo pela orientação dada nesta trabalho, partilha de conhecimento científico e apoio fundamental na resolução de problemas, mesmo quando pensei que estes não teriam resolução.

-À Técnica Coordenadora Isabel Diegues pelos sábios conselhos e experiência, que nunca hesitou partilhar comigo. Agradeço não só o apoio a nível profissional, mas também emocional, que se revelou essencial como uma base de apoio para toda a realização do trabalho. Gostaria também de agradecer, igualmente à Técnica Sub-Coordenadora Céu Raimundo.

-À Coordenadora do Departamento de Física Médica do HSM, Doutora Esmeralda Poli, por me ter concedido autorização para realizar o trabalho no departamento. Se não ultrapassasse esta fase, uma grande parte do trabalho não passaria de uma simples ideia.

-Especialmente, ao Eng. Luís Madureira pela ajuda na aquisição de dados CTDI, Téc. Ana Duarte e Téc. Ana Rato pela ajuda na elaboração de distribuições de dose no sistema de planeamento. Agradeço aos três pelas horas de trabalho que dispensaram comigo, principalmente à Téc. Ana Duarte, cujas noites passadas em claro e fins-de-semana no Serviço a ajudar-me foram cruciais e de um valor absolutamente incalculável.

-Às minhas colegas, Téc. Rita Lourenço, Téc. Isabel Caetano, Téc. Catarina Marques, Téc. Sandra Cabral, Téc. Sandra Lemos, Téc. Vera Quintino, Téc. Marta Rocha, Téc. Dagmar Parreira, Téc. Sara Brito, Téc. Adriana Borges, Téc. Mayra Pereira, Téc. Mafalda Ferreira e Téc. Inês Lima, pela aquisição de dados para o trabalho.

- À Professora Elisabete Carolino pelo esclarecimento de dúvidas na análise estatística.

-À Dra. Joana Pinto pelo suporte prestado no esclarecimento de dúvidas, acerca da estação de trabalho XVI®.

-Ao meu noivo Miguel Reis Ferreira pelo apoio prestado a nível pessoal e científico, mas principalmente pelo suporte emocional, deveras importante para ter conseguido levar a cabo este trabalho.

-À minha mãe e ao meu padrasto Zé Maria, responsáveis pelo meu sucesso profissional e pessoal ao longo dos anos e que mais uma vez me apoiaram sem qualquer reserva.

-Aos amigos Adriana Nogueira, Ana Rodrigues, Ana Martins, Carlos Pedroso e Fernando Almeida, por me acompanharem em todos os momentos, especialmente pelas visitas que me fizeram nos dias mais difíceis pelos quais passei nesta fase.

Muito Obrigada a todos,
Espero um dia poder retribuir todo o apoio prestado.
Rita Simões, Dezembro 2011.

INTRODUCTORY NOTE

Precision is an imperative in modern radiotherapy. This concept is applied in a day-to-day basis at all levels in planning and delivering treatment to patients, since only by uniting all these aspects is it's real application possible.

Given that I am a radiation technologist in an institution where the purpose is to ensure accuracy in administered treatment, my main focus was to direct this work towards the field in which I dwell daily. Indeed, making sure that all instruments available have a precisely studied role in the quality of the execution of prescribed treatment has become a necessity that justifies the enormous amount of care put in the treatment phase in radiotherapy. This applies, namely, to the recently-implemented cone-beam computed tomography (CBCT) tool. Therefore, computerized tomography dose indices (CTDI) were acquired in order to monitor doses administered to patients through CBCT. This was followed by the selection of twenty one patients of pathologies involving a great amount of precision: fourteen patients with prostate and seven patients with head and neck tumours. This sample was characterized with the acquisition of CBCT pre and post-treatment, as well as after any correction performed on their positioning. This allowed for evaluating intra-fraction errors.

From within this sample, patients out of action limits were chosen, as analyzed in control charts for mean and standard deviation of their positioning deviations, as well as patients out of tolerance limits for deviation correction.

Finally, new dosimetric distributions were performed, in which the isocenter accounts for the measured positioning errors. The doses in organs at risk and eventual differences in planning target volume (PTV) coverage with 95% of the dose between these and the planned distributions were compared for each of these patients. This simulation allowed for inferring what would have happened had these errors not been accounted for and corrected.

This study also evaluated the feasibility of using CBCT in the imaging verification during the treatment of patients with the aforementioned pathologies, as well as the adequacy of the image acquisition protocol, as currently implemented at the department. The evaluation and quantification of systematic and random translational and rotational errors was also made possible, as defined by current departmental practices. This allowed for adapting not only the mentioned protocol, but also margins currently added to clinical target volumes (CTV) for PTV generation. This will allow to ensure that protocols are based on data obtained locally, which will undoubtedly procure better results in cancer healthcare at the department.

It is noteworthy that the Master Comission authorized the presentation of this work as a scientific article, with the purpose of future publication in international, peer-reviewed

journals. In order to do so, it is not only written in English, but it also respects criteria related to this objective.

In the first part, a review on state-of-the-art literature is rendered (previously submitted in May 2011, even though some aspects have been corrected or updated), as to allow for a contextualization of my work. The feasibility of the IGRT protocol, as implemented at my department, is then assessed. Finally, as previously discussed, systematic and random translational and rotational errors are evaluated.

INDEX

DESVIO DE POSICIONAMENTO EM RADIOTERAPIA PARA PATOLOGIAS DE CABEÇA E PESCOÇO E PRÓSTATA: REVISÃO DE LITERATURA

RADIOTHERAPY SETUP DEVIATIONS IN HEAD AND NECK AND PROSTATE TUMOURS: A REVIEW

(TITULO ABREVIADO: DP EM CP E PRÓSTATA: REVISÃO DE LITERATURA)

ANA RITA SIMÕES[1], MARGARIDA EIRAS[2], ISABEL MONTEIRO GRILLO[1].

1-SERVIÇO DE RADIOTERAPIA, HOSPITAL DE SANTA MARIA, CENTRO HOSPITALAR LISBOA NORTE, EPE.
2-ESCOLA SUPERIOR DE TECNOLOGIA DA SAÚDE DE LISBOA.

RESUMO

INTRODUÇÃO: Numa era em que os tratamentos de Radioterapia Externa (RTE) exigem cada vez mais precisão, a utilização de imagem médica permitirá medir, quantificar e avaliar o impacto do erro provocado pela execução do tratamento ou pelos movimentos dos órgãos. **OBJECTIVO:** Analisar os dados existentes na literatura acerca de desvios de posicionamento (DP) em patologias de Cabeça e Pescoço (CP) e próstata, medidos com *Cone Beam Computed Tomography* (CBCT) ou *Electronic Portal Image Device (EPID).* **METODOLOGIA:** Para esta revisão da literatura foram pesquisados artigos recorrendo às bases de dados *Medline/Pubmed e B-on*. Foram incluídos artigos que reportassem DP em patologias CP e próstata medidos através de CBCT e EPID. Seguidamente foram aplicados critérios de validação, que permitiram a selecção dos estudos. **RESULTADOS:** Após a análise de 35 artigos foram incluídos 13 estudos e validados 9 estudos. Para tumores CP a média (μ) dos DP encontra-se entre 0,0 e 1,2 mm, com um desvio padrão (σ) máximo de 1,3mm. Para patologias de próstata observa-se μ_{DP} compreendido entre 0,0 e 7,1 mm, com σ máximo de 7,5mm. **DISCUSSÃO/ CONCLUSÃO:** Os DP em patologias CP são atribuídos, maioritariamente, aos efeitos secundários da RTE, como mucosite e dor, que afectam a deglutição e conduzem ao emagrecimento, contribuindo para a instabilidade da posição do doente durante o tratamento, aumentando as incertezas de posicionamento. Os movimentos da próstata devem-se principalmente às variações de preenchimento vesical, rectal e gás intestinal. O desconhecimento dos DP afecta negativamente a precisão da RTE. É importante detectá-los e quantificá-los para calcular margens adequadas e a magnitude dos erros, aumentando a precisão da administração de RTE, incluindo o aumento da segurança do doente.

PALAVRAS CHAVE: Desvios de posicionamento, Cone-Beam CT, EPID, Precisão.

ABSTRACT:

BACKGROUND AND PURPOSE: In an era where precision is an increasing necessity in external radiotherapy (RT), modern medical imaging techniques provide means for measuring, quantifying and evaluating the impact of treatment execution and movement error. The aim of this paper is to review the current literature on the quantification of setup deviations (SD) in patients with head and neck (H&N) or prostate tumors, using Cone Beam Computed Tomography (CBCT) or Electronic Portal Image Device (EPID). **METHODS:** According to the study protocol, *Medline/Pubmed* and *B-on* databases were searched for trials, which were analyzed using selection criteria based on the quality of the articles. **RESULTS:** After assessment of 35 papers, 13 studies were included in this analysis and nine were authenticated (6 for prostate and 3 for H&N tumors). The SD in the treatment of H&N cancer patients is in the interval of 0.1 to 1.2 mm, whereas in prostate cancer this interval is 0.0 to 7.1 mm. **DISCUSSION:** The reproducibility of patient positioning is the biggest barrier for higher precision in RT, which is affected by geometrical uncertainty, positioning errors and inter or intra-fraction organ movement. There are random and systematic errors associated to patient positioning, introduced since the treatment planning phase or through physiological organ movement. **CONCLUSION:** The H&N SD are mostly assigned to the Radiotherapy adverse effects, like mucositis and pain, which affect swallowing and decrease secretions, contributing for the instability of patient positioning during RT treatment and increasing positioning uncertainties. Prostate motion is mainly related to the variation in bladder and rectal filling. Ignoring SD affects negatively the accuracy of RT. Therefore, detection and quantification of SD is crucial in order to calculate appropriate margins, the magnitude of error and to improve accuracy in RTE and patient safety.

KEYWORDS: Set-up deviation, Cone-Beam CT, EPID, Accuracy.

1. INTRODUÇÃO

O objectivo primordial da Radioterapia Externa (RTE) é a administração de uma dose de radiação, medida com precisão, num volume tumoral definido, com o mínimo possível de efeitos secundários nas células vizinhas. Com este método de tratamento, pretende-se a erradicação do tumor, elevada qualidade de vida e prolongamento da sobrevivência.[1]

De maneira a tornar este objectivo real e exequível, com o menor número de imprecisões, foram definidas incertezas e fontes de erro em RTE associadas à preparação e administração do tratamento. Sabe-se, então, que as fontes de introdução de incertezas estão principalmente relacionadas com incertezas de posicionamento do doente, assim como com a delimitação do *Gross Tumor Volume*

(GTV), devendo-se esta última ao desconhecimento da extensão microscópica do tumor. [2-8,10]

Centrar-nos-emos, neste trabalho, na análise das incertezas de posicionamento, nomeadamente dos desvios de posicionamento (DP) do doente durante o tratamento de radioterapia. São estes definidos como diferenças anatómicas observáveis através da comparação de uma imagem de referência com uma imagem prévia ao tratamento.[10-13]

Atendendo à dimensão desta problemática e centrando-nos numa Era em que a precisão é cada vez mais exigida, a utilização de imagem médica permitirá medir, quantificar e avaliar o impacto dos DP na execução do tratamento ou no erro provocado pelos movimentos dos órgãos de uma forma mais precisa. Nesse sentido, tem-se verificado, nas últimas décadas, um claro aumento do investimento na tecnologia utilizada nesta área. Tornou-se assim comum a introdução de protocolos de verificação imagiológica com recurso a ferramentas como o *Electronic Portal Image Device* (EPID) ou a *Cone Beam Computed Tomography* (CBCT) nos departamentos de radioterapia a nível mundial.

A utilização de EPID para verificação do posicionamento do doente revelou-se um método eficaz, substituindo a utilização de filmes radiográficos em Radioterapia. Tal, deve-se, ao facto de estas imagens digitais, obtidas através de um detector de silício amorfo, terem um maior contraste e uma qualidade marcadamente superior. Ao recorrermos a este método, os DP são baseados, principalmente, na anatomia óssea, facilmente observada em duas dimensões (2D).[14]

Com o intuito de aumentar a precisão da Radioterapia, surge o CBCT, com a possibilidade de realizar imagens volumétricas, associadas a uma boa visualização de tecidos moles, baixas doses de radiação e possibilidade de observar variações inter e intrafracção.[15] Este sistema é baseado numa fonte de raios x posicionada no sentido oposto do detector, posicionada no anel do acelerador linear. Enquanto a *gantry* roda à volta do doente, a reconstrução da imagem é obtida através de uma aproximação bidimensional dos dados de projecção.[3]

Tendo em conta esta realidade, o presente trabalho pretende analisar a literatura existente acerca de DP em doentes com patologias de Cabeça e Pescoço (CP) e próstata, medidos com CBCT ou EPID.

2. METODOLOGIA

2.1 PESQUISA DE ARTIGOS

Para esta revisão de literatura foram pesquisados artigos recorrendo às bases de dados *Medline/Pubmed* e *B-On*, através das palavras *Cone-Beam CT*, *EPID*, *Head and Neck*, *Prostate*, *Intrafraction errors*, *intrafraction errors* e *setup error*. A pesquisa foi limitada a publicações escritas em Inglês.

Parâmetros de avaliação dos estudos	Classificação
1. Materiais e métodos explicados	5
2. Dados dos desvios disponíveis:	
a) Dados em bruto	3
b) Média, desvio padrão, medida de tendência central	2
3. Descrição da metodologia de análise dos DP e erros aleatórios e sistemáticos	3
4. Avaliação dos erros de setup segundo um protocolo de aquisição de imagem	2
5. Dimensão da amostra:	
a) 6 a 10 doentes	2
b) 11 ou mais doentes	3
6. Conformidade entre objectivo e métodos utilizados	5
7. São quantificados DP?	5
8. Existe análise dos desvios de posicionamento?	5
9. É apresentado um significado clínico para os DP?	5
10. É um estudo prospectivo?	5
11. A conclusão está em conformidade com o objectivo proposto?	5
12. São sugeridas estratégias para diminuição do erro sistemático?	3
13. Um dos objectivos é definição de protocolo ou linhas de orientação para implementação?	3
14. Existe uma preparação prévia ao tratamento?	4
15. Descrição da preparação, se aplicável.	3
16. Uniformidade do posicionamento dos doentes.	2
17. Consentimento informado	1
Classificação máxima:	62

Tabela 1: Parâmetros de validação dos estudos incluídos.

2.2 SELECÇÃO DE ARTIGOS

Foram incluídos artigos que quantificassem DP de doentes com tumores malignos de próstata ou localizados na região de CP submetidos a tratamentos RTE. Destes, foram seleccionados os estudos cujos DP foram avaliados através das ferramentas de aquisição de imagem CBCT ou EPID.

Em alguns dos estudos foram apenas seleccionados os dados referentes às patologias de próstata e patologias de CP, sendo excluídos todos os DP existentes referentes a outras patologias.

Autor	Ano	Posicionamento	Amostra	Ferramenta de aquisição de imagem
Xu et al[21]	2008	Dec. Dorsal; Acessório de fixação de mascaras; máscara termoplástica de cabeça; depressor de ombros; apoio popliteu.	n=19	CBCT
Wang et al[23]	2009	Dec. Dorsal; Acessório de fixação de mascaras; máscara termoplástica de cabeça; apoio popliteu.	n=22	CBCT
Xu et al[22]	2009	Dec. Dorsal; Acessório de fixação de mascaras; máscara termoplástica de cabeça; depressor de ombros; apoio popliteu.	n=19	CBCT

Tabela 2 : Representação por autor, ano, posicionamento, ferramenta de aquisição de imagem dos estudos de patologias de CP considerados para este trabalho.

2.3 ESTRATÉGIAS DE SELECÇÃO DE ARTIGOS

Para a presente revisão, foram definidos parâmetros de avaliação da qualidade dos estudos incluídos, tal como descritos por Jadad et al.[17]

Elaborou-se uma tabela (tabela1) com os itens considerados como desejavelmente descritos nos artigos. De seguida, foi verificada a conformidade entre os parâmetros definidos e os descritos nos estudos. Caso os itens estivessem descritos, seria atribuída a classificação designada. A classificação máxima estimada para os artigos incluídos foi de 62 pontos. Foram excluídos todos os estudos que obtiveram uma classificação inferior ou igual a 29 pontos, cujos dados de DP não estivessem quantificados e cuja amostra fosse inferior a 5 doentes.

Após terem sido incluídos 13 estudos para esta revisão foram validados 9 estudos (3 referentes a tumores de CP e 6 a patologias de próstata). A pontuação média obtida

no processo de validação dos estudos foi de 39,1 pontos, com amplitude de 31 a 49 pontos.

Na tabela 2 e 3 encontram-se descritos os estudos e algumas das suas características.

Nairz et al.[26]	**2008**	**Não especificado**	**n=27**	**Não**	**Não**	**CBCT**
Aubry et al.[29]	2004	Não especificado	n=18	Sim	Bexiga Cheia e recto vazio	EPID
Sandhu et al.[27]	2008	Dec. Dorsal; colchão de vácuo.	n=26	Sim	Bexiga Cheia e recto vazio	EPID
Polat et al.[28]	2008	Não especificado	n=27	Não	Bexiga Cheia e recto Vazio. Aconselhamento nutricional.	CBCT
Chueng et al.[30]	2005	Dec. Dorsal; colchão de vácuo.	n=33	Sim	Bexiga e recto vazios	EPID
Rajendran et al.[31]	2010	Dec. Dorsal; apoio região pélvica e região politeia	n=28	Sim	Bexiga cheia	EPID

Tabela 3 : Representação por autor, ano, posicionamento, dimensão da amostra, marcadores fiduciais, preparação e ferramenta de aquisição de imagem dos estudos de patologias de próstata considerados.

3. RESULTADOS

3.1. DESVIOS DE POSICIONAMENTO

3.1.1. CABEÇA E PESCOÇO

Na tabela 4 encontram-se descritos os resultados, da média (μ_{DP}) e desvio padrão (σ_{DP}) dos DP dos mesmos autores. Wang et al. documentaram que a μ_{DP} se encontrava entre 0,0 e 0,7 mm, enquanto o intervalo de σ_{DP} é de 0,4 a 1,3 mm. Xu et al. registou, em 2008, valores de μ_{DP} entre 0,6 e 1,2 mm com σ_{DP} entre 0,5 e 1,1mm. Em 2009, o mesmo autor publicou um estudo cujos doentes apresentavam DP entre 0,1 e 0,3 mm, com σ entre 0,4 e 0,8 mm.

AUTOR	DP (MÉDIA ± DESVIO PADRÃO) SENTIDOS		
	Latero-medial (X)	Cranio-caudal (Y)	Antero-Posterior (Z)
Wang et al.[23]	-0,7±1,1 -0,4±0,5 -0,3±0,7	-0,7±1,3 0,3±0,5 0,3±0,9	-0,3±1,2 0,0±0,4 0,1±0,7
Xu et al.[22]	-0,3±0,5 -0,3±0,6	0,1±0,5 0,3±0,8	0,2±0,4 0,2±0,6
Xu et al.[21]	1,2±0,9 1,2±1,1 1,0±0,8	0,7±0,6 0,6±0,5 0,6±0,5	0,9±0,8 1,0±0,9 0,9±0,7

Tabela 4: Representação dos DP (média ± desvio padrão) para patologias de CP.X,Y e Z, representam, respectivamente, os sentidos latero-medial, crânio-caudal e antero-posterior.

3.1.2. PRÓSTATA

Na tabela 5 encontram-se descritos os resultados dos autores. Nairz et al. documentaram que o μ_{DP} se encontrava entre 0,0 e 0,7 mm, enquanto o intervalo de σ_{DP} é de 1,6 a 3,4 mm. Aubry et al. registou valores de μ_{DP} entre 0,0 e 0,2 mm com σ_{DP} entre 0,2 e 0,7mm. Sandhu et al publicou DP entre 1,0 e 5,3 mm, com σ_{DP} entre 1,7 e 8,1 mm. Polat et al. analisou, apenas, os DP no sentido antero-posterior, e foi obtida μ_{DP}=0 mm, para todas as aquisições, os valores de σ_{DP} encontraram-se entre 1,0 e 1,7mm, enquanto que para Cheung et al., a média dos DP foi quantificada entre 0,14 e 0,72mm. Rajendram et al. registou um μ_{DP} entre 0,7 mm e 7,1mm.

Os valores mais elevados de DP, para estas patologias encontram-se no sentido antero-posterior.

4. DISCUSSÃO

A reprodutibilidade do posicionamento do doente é a maior barreira para o aumento da precisão em Radioterapia, que é afectada por múltiplos aspectos inerentes ao tratamento.[13,24,25] Nesse sentido, caracterizam-se os DP como o somatório de erros sistemáticos (introduzidos ao longo do planeamento), erros aleatórios (associados a cada fracção) e de incertezas geométricas (relacionadas com o equipamento).[6]

Para CP, observa-se que a média dos DP tem uma amplitude entre 0,0 e 1,2 mm, com um desvio padrão máximo de 1,3 mm. É ainda de referir que os resultados dos não diferem significativamente na literatura consultada, o que poderá ser atribuído à utilização de máscara de imobilização. Nestes estudos, o aumento dos

Autor	DP (média±desvio padrão)		
	S.Latero-Medial (X)	S. Craneo-caudal (Y)	S.Antero-posterior (Z)
Nairz et al.[26]	0,0±1,6	0,0±2,4	0,7±3,4
Aubry et al.[29]	0,2±0,2	0,0±0,4	0,2±0,7
Sandhu et al.[27]	3,9±5,9 1,0±1,7 3,6±5,6	5,3±8,1 2,4±2,1 4,9±7,5	3,8 ±5,5 2,8±2,1 5,2±7,1
Polat et al.[28]	Não foi avaliado	Não foi avaliado	0±1,7 0±1,0 0±1,3
Chueng et al.[30]	0,14±0,9	0,45±1,3	0,72±1,8
Rajendran et al.[31]	0,8±6,8	4,2±4,9	7,1±7,4

Tabela 5: Representação dos DP(média ± desvio padrão), em mm, para patologias de Próstata. X,Y e Z, representam, respectivamente, os sentidos latero-medial, crânio-caudal e antero-posterior.

DP no decorrer da RTE é relacionado com o aparecimento de efeitos secundários do tratamento, nomeadamente mucosite e xerostomia. De facto, com o aparecimento destes sintomas, a deglutição é afectada, conduzindo a perda ponderal. Se somarmos a este factor a dor inerente ao desenvolvimento de inflamação nos tecidos durante o tratamento, compreende-se que o posicionamento do doente sofre de uma maior imprecisão e menor reprodutibilidade. [21-23]

Nesta análise verifica-se que os DP em doentes com patologia de CP são menores do que no caso de doentes com patologia prostática. No entanto, não devemos descurar o seu estudo e medição, já que existem valores atípicos para alguns doentes que deverão sempre ser corrigidos.

Os DP da próstata devem-se principalmente a variações de preenchimento vesical e rectal. Observa-se que a média dos DP para próstata tem uma amplitude de 0,0 e 7,1 mm, com um desvio padrão máximo de 7,5mm. Os menores valores de DP são reportados por Polat et al., apresentando-se no sentido antero-posterior. Tal poderá estar relacionado com o facto de o aconselhamento nutricional, aplicado por estes autores, ser um factor essencial para o controlo da posição do recto e, consequentemente, da próstata. É assim realçada a importância da implementação de um protocolo que englobe esta componente, além da necessária preparação de bexiga e recto. Note-se que apenas um autor desconsiderou a preparação rectal e vesical.[26]

É ainda de referir que não existe unanimidade na literatura em relação ao procedimento que deverá ser realizado para controlar o volume da bexiga. Alguns autores referem instruir os doentes para ingerir sempre a mesma quantidade de água antes do tratamento. Contudo, na maioria dos artigos analisados não é descrita a quantidade de água nem o tempo de espera antes de realizar tratamento. Por outro lado, Chueng et al. defendem que a bexiga e o recto deverão estar vazios antes do tratamento para que se possa controlar o movimento interno da próstata de uma forma precisa.

Verifica-se ainda que os autores que utilizam CBCT não colocam marcas radiopacas na próstata, apesar de não ser referida uma justificação. Sugere-se que o motivo desta observação se prende com a visualização de tecidos moles nas imagens de CBCT. Apesar da visualização da próstata se manter inexacta ao recorrer a tomografia computorizada, é muito mais precisa quando comparada com EPID, onde apenas são visíveis estruturas ósseas. É ainda de referir que os quatro autores analisados que utilizam EPID, recorrem à utilização de marcadores fiduciais.

Os DP apresentados nos estudos que contemplam a patologia de próstata poderão não ser comparáveis, uma vez que se verificam diferenças no posicionamento utilizado para os doentes de próstata entre os diversos autores.

5. CONCLUSÃO

O desconhecimento dos DP afecta negativamente a precisão da radioterapia, pelo que a detecção e quantificação dos primeiros permitirá o aumento da última. De facto, conhecer o DP para cada patologia em cada centro de Radioterapia permitirá calcular o erro sistemático e aleatório associado à localização de tratamento. Tal permitirá não só calcular margens de tratamento adequadas, mas também definir protocolos de aquisição de imagem. Esta abordagem levará a um incremento da precisão e diminuição das incertezas no tratamento. Aumentar-se-á, consequentemente, a sua qualidade de administração.

Verifica-se existirem mais estratégias de redução de DP para a patologia de próstata do que para CP. Esta diferença decorrerá potencialmente dos valores de DP documentados para CP serem relativamente diminutos quando comparados com os DP de patologias próstaticas. No entanto, entende-se que para CP é desejável o desenvolvimento de estratégias que minimizem a toxicidade da RTE. Tal como

anteriormente referido, a toxicidade do tratamento provoca queixas álgicas e evolução da morfologia (com a perda ponderal) do doente, tornando-a, segundo os autores, na maior fonte de DP durante o tratamento.

Verificam-se, presentemente, grandes discrepâncias na forma de apresentar estes resultados na literatura. Futuramente dever-se-ão definir linhas de orientação que permitam uma definição uniforme e inequívoca de como quantificar DP com os vários métodos disponíveis. Deverão ser sempre tomados em conta aspectos como a ferramenta de imagem usada, os momentos da sua utilização, a definição de um eventual protocolo nutricional e/ou de preparação de órgãos de risco e o método de análise dos vários parâmetros. A instituição de uma homogeneização dos dados publicados permitiria, no futuro, análises metodológicas mais claras e a potenciação do desenvolvimento de melhores estratégias no caminho para o aumento da precisão em radioterapia.

6. REFERÊNCIAS BIBLIOGRÁFICAS

1. Perez C. Principles and practice of Radiation Oncology. Lipincott Williams & WillKins; 2008.

2.Verellen D., Ridder M., Storme G. A (short) history of image-guided radiotherapy. Radiotherapy and Oncology. 2008;86:4–13.

3.Verellen D., Ridder M., Tournel K., Duchateau M., Reynders T., Gevaert T., Linthout N., Storme g. An overview of volumetric imaging technologies and their quality assurance for IGRT. Acta Oncologica 2008;47:1271-1278.

4.Olsen D., Thwaites D. Now you see it… Imaging in radiotherapy treatment planning and delivery. Radiotherapy and Oncology 2007;85:173-175

5.Xing L., Thorndyke B., Schreibmann E., Yang Y., Li T., Kim G., Luxton G., Koong A. Overview of image-guided Radiation Therapy. Medical Dosimetry 2006;31:91-112.

6.Van Herk M. Errors and Margins in Radiotherapy. Seminars in Radiation Oncology 2004;14(1):52-64.

7.Mansson S. Patient positioning correction strategies in radiotherapy: A portal imaging study [Master thesis]. Lund: Lund University; 2004.

8.Van Herk M., Remeijer P., Rasch C., Lebesque J. The Probability of correct target dosage: Dose-population histograms for deriving treatment margins in Radiotherapy. Int J Radiation Oncology Biol Phys 2000;47(4):1121–1135.

9.Kukołowicz P. ICRU 50 & ICRU 62. In: Summer School of Radiotherapy, 2003, Kielce, Poland. Available from: http://www.pptsearch.net/details-icru-50-amp-icru-62-129640.html

10.Langen K., Jones T. Organ Motion and its Management. Int J Radiation Oncology Biol Phys 2001;50(1):265–278.
11.Yan, D., Lockman, D., Martinez, A., Wong ,J., Brabbins D., Vicini,F., Liang, J., Kestin, L. Computed Tomography Guided Management of Interfractional Patient Variation. Semin Radiat Oncol 2005;15:168-179.
12.ICRU Report 62. International Commission on Radiation Units and Measurements. Prescribing, recording and reporting photon beam therapy. Supplement to ICRU Report 50; 1999.
13.Kupelian P., Langen K., Willoughby T., Zeidan O., Meeks S. Image-Guided Radiotherapy for Localized Prostate Cancer: Treating a Moving Target. Seminars in Radiation Oncology 2008;18:58-66.
14.Herman M. Clinical use of portal imaging. Seminars in Radiation Oncology. 2005;15(3):157-67.
15.Oldham M., Le´tourneau D., Watt L., Hugo G., Yan D.,Lockman D., Kim L., Chen P., Martinez A., Wong J. Cone-beam-CT guided radiation therapy: A model for on-line application. Radiotherapy and Oncology. 2005;75(3):271-8.
16.Cook D., Mulrow C., Haynes R. Systematic Reviews: Synthesis of Best Evidence for Clinical Decisions. Annals of Internal Medicine 1997;126:376-380.
17.Jadad A., Moore R., Carroll D., Jenkinson C., Reynolds D., Gavaghan D., McQuay H. Assessing the Quality of Reports of Randomized Clinical Trials: Is Blinding Necessary? Controlled Clinical Trials 1996;17:1-12.
18.Green J. Cochrane Handbook for Systematic Reviews of Interventions - Cochrane Book Series. The Cochrane Collaboration and John Wiley & Sons; 2008.
19. Ramalho A. Redacção de estudos e projectos de revisão com e sem metanálise. Coimbra: formasau; 2005.
20.Huang E., Dong L., Chandra A., Kuban D., Rosen I., Evans A., Pollack A. Intrafraction prostate motion during IMRT for Prostate Cancer. Int J Radiation Oncology Biol Phys 2002; 53(2):261–268.
21.Xu F., Wang J., Bai S., Xu Q., Shen Y., Zhong R. Interfractional and intrafractional setup errors in radiotherapy for tumors analyzed by cone-beam computed tomography. Chinese Journal of Cancer 2008;27(10):372-376.
22.Xu F., Wang J., Bai S., Li Y., Shen Y., Zhong R., Jiang X., Xu Q. Detection of intrafractional tumour position error in radiotherapy utilizing cone beam computed tomography. Radiotherapy and Oncology 2009;89:311–319.
23.Wang J., Bai S., Chen N., Xu F., Jiang X., Li Y., Xu Q., Shen Y., Zhang H., Gong Y., Zhong R., Jiang Q. The clinical feasibility and effect of online cone beam computer

tomography-guided intensity-modulated radiotherapy for nasopharyngeal cancer. Radiotherapy and Oncology 2009;90:221–227.
24.Smitsmans M., Pos F, Bois J., Heemsbergen W., Sonke J., Lesbesque J., Van Herk M. The influence of a dietary protocol on Cone Beam CT-Guided Radiotherapy For Prostate Cancer Patients. Int J Radiation Oncology Biol Phys 2008;71(4):1279–1286.
25.Rosewall T., Chung P., Bayley A., Lockwood G., Bristow R., Kong V., Milosevic M., Catton C. A randomized comparison of interfraction and intrafraction prostate motion with and without abdominal compression. Radiotherapy and Oncology 2008;88:88–94.
26.Nairz O, Merz F, Deutschmann H, Kopp P, Schöller H, Zehentmayr F, Wurstbauer K, Kametriser G, Sedlmayer F. A strategy for the use of image-guided radiotherapy (IGRT) on linear accelerators and its impact on treatment margins for prostate cancer patients. Strahlenther Onkol. 2008;184(12):663-7.
27.Sandhu A., Sethi R., Rice R., Wang J., Marcus L., Salem C.,Downs T., Kellogg J., Millard F., Pawlicki T., Mundt A. Prostate bed localization with image-guided approach using on-board imaging: Reporting acute toxicity and implications for radiation therapy planning following prostatectomy. Radiotherapy and Oncology 2008;88:20–25.
28.Polat B., Guenther I., Wilbert J., Goebel J., Sweeney R., Flentje M.,Guckenberger M. Intra-Fractional Uncertainties in Image-Guided Intensity-Modulated Radiotherapy (IMRT) of Prostate Cancer. Strahlenther Onkol 2008;184:668–73
29.Aubry F., Beaulieu L., Girouard L., Aubin S., Tremblay D., Laverdière J., Vigneault E. Measurements of intrafraction motion and interfraction and intrafraction rotation of prostate by three-dimensional analysis of daily portal imaging with radiopaque markers. Int J Radiat Oncol Biol Phys. 2004;60(1):30-9.
30.Cheung P., Sixel K., Morton G., Loblaw D., Tirona R., Pang G., Choo R., Szumacher E., Deboer G., Pignol J. Individualized planning target volumes for intrafraction motion during hypofractionated intensity-modulated radiotherapy boost for prostate cancer. Int J Radiat Oncol Biol Phys. 2005;62(2):418-25.
31.Rajendran R., Plastaras J., Mick R., McMichael Kohler D., Kassaee A., Vapiwala N. Daily isocenter correction with electromagnetic-based localization improves target coverage and rectal sparing during prostate radiotherapy. Int J Radiat Oncol Biol Phys. 2010;76(4):1092-9.
32.Skarsgard D., Cadman P., El-Gayed A., Pearcey R., Tai P., Pervez N., Wu J. Planning target volume margins for prostate radiotherapy using daily electronic portal imaging and implanted fiducial markers. Radiation Oncology 2010;5:52.
33.Huang E, Dong L, Chandra A, Kuban DA, Rosen II, Evans A, Pollack A. Intrafraction prostate motion during IMRT for prostate cancer. Int J Radiat Oncol Biol Phys 2002;53(2):261-8.

34.Létourneau D, Martinez AA, Lockman D, Yan D, Vargas C, Ivaldi G, Wong J. Assessment of residual error for online cone-beam CT-guided treatment of prostate cancer patients. Int J Radiation Oncology Biol Phys 2005;62(4):1239–1246.
35.Takemura A, Shoji S, Ueda S, Kurata Y, Kumano T, Takamatsu S, Suzuki M. Effect of daily setup errors on individual dose distribution in conventional radiotherapy: an initial study. Radiol Phys Technol 2009;2(2):151-8.

THE FEASIBILITY OF AN IGRT PROTOCOL

ANA RITA SIMÕES[1], MARGARIDA EIRAS[2], ISABEL MONTEIRO GRILLO[1].

1-SERVIÇO DE RADIOTERAPIA, HOSPITAL DE SANTA MARIA, CENTRO HOSPITALAR LISBOA NORTE, EPE.
2-ESCOLA SUPERIOR DE TECNOLOGIA DA SAÚDE DE LISBOA.

BACKGROUND/PURPOSE: Treatment accuracy and reproducibility are important issues in radiotherapy. In order to minimize uncertainties, implementation of Image-Guided Radiotherapy(IGRT) has become an imperative. This work is intended to discuss and assess the feasibility of an implemented IGRT protocol in a radiotherapy department, for prostate and Head ans Neck(HN) patients, with the use of Cone-Beam Computed Tomography(CBCT).

MATERIAL/METHODS: Computed Tomography Dose Indices(CTDI) were measured in a phantom to preview the delivered doses with CBCT. A sample of 21 patients(pts) was then selected, composed of 14 pts with prostate and 7 pts with HN tumours. CBCT images were subsequently acquired from pts. Dose distributions were performed for 6 prostate and 6 head and neck pts, chosen according to setup deviation magnitude in control charts.

RESULTS: The administered doses ranged from 9,18mGy to 15,76mGy for HN and from 170,7mGy to 528,8mGy. Differences in Prostate PTV were:-40,3cc to 2,8cc for PTV1; -22,3cc to -4cc for PTV2 and -8,1cc to -2,7cc for PTV3. For HN pts the differences in dose distributions ranged from -7,4cc to 3,3cc for PTV1 and from -5,1cc to 0.8 cc for PTV2.

CONCLUSIONS: The IGRT protocol is feasible, safe and yields a clear therapeutic gain for pts with HN and prostate tumours. Future work should be aimed at accounting for the dose delivered with CBCT at the treatment planning level.

ADVANCES IN KNOWLEDGE: A new evaluation method for IGRT protocol efficacy, that takes into account setup error corrections dosimetrically, is described. According to it, increased dose administered by CBCT is justified.

INTRODUCTION

With the emergence of new dose-delivering techniques in the 1990s, such as radiosurgery and Intensity Modulated Radiotherapy (IMRT), treatment accuracy and reproducibility in

Rdiotherapy (RT) became a crucial issue.[1-4] In order to minimize positioning uncertainties, previously described by several authors, implementation of imaging tools for treatment verification has become an imperative. [5-8]

The utilisation of Imaged-guided Radiotherapy (IGRT) protocols has been precisely described in the literature in several instances, as has the use of imaging tools in the treatment room to evaluate and correct set-up deviation (SetD). One of these tools is the Cone Beam Computed Tomography (CBCT), which allows the tridimensional verification of patient anatomy, enabling visualization of the tumour and surrounding structures. It is thus possible to adjust patient positioning immediately before treatment, detecting gross errors, eliminating systematic errors and reducing random errors.[9-13] The implementation of an IGRT protocol, using CBCT, allows for a predicted increase in the clinical benefit of radiotherapy, since monitoring organ motion, verification of tumour volume movement, size and position, and control position error are thus made possible.[7,14-20]

However, there is a foreseeable consequence: the administered dose is increased by image acquisition during treatment. The Report of the American Association of Physicists in Medicine (AAPM) Task Group 75 recommends that the risk of increasing dose has to be weighed against the eventual increase in precision during treatment delivery.[21]

In accordance with this paradigm, the feasibility of the imaging verification protocol for prostate and head and neck tumours using CBCT, implemented at our department, is hereby analysed, we verify an eventual clinical benefit that, may, outweigh the aforementioned dose increment. In order to accomplish this purpose, Computed Tomography Dose Index (CTDI) values were measured in a phantom so as to preview the delivered doses with CBCT acquisition. CBCT images were subsequently acquired from patients. Doses distributions were then performed in a Treatment Planning System (TPS), taking into account the setup deviation (SetD) measured in patients, with the objective of simulating what would be the predictible scenario if the deviations had not been corrected.

METHODS AND MATERIALS

As aforementioned, the main objective of the work hereby reported was the evaluation of the feasibility of the IGRT protocol currently implemented at our department. CTDI measurements inherent to the acquisition of CBCT imaging were quantified for prostate and HN pathologies with the different filters and collimators of the Beam Modulator ^{TM} (ELEKTA Oncology Systems,Crawley, UK) linear accelerator. A sample of 21 patients 7 with HN and 14 with prostate tumours) was subsequently selected. Pre-treatment imaging was acquired in accordance with the IGRT protocol, and by using control charts, pts with SetD out of statistic

control were identified. Dosimetric distributions were performed for the latter patients to evaluate the impact of the SetD in case these would not have been corrected.

Kilovoltage X-ray IGRT system

CTDI measurements were made in a Beam Modulator™ (ELEKTA Oncology Systems, Crawley, UK) linear accelerator using CBCT protocols integrated into the X-Ray Volume Imaging (XVI®) software as described by several authors. [22-24] The XVI® system (release 4.2.1) consists of a conventional x-ray tube mounted on a retractable arm and a kV detector planel, itself mounted on the drum of the digital accelerator. The tube was located 1000mm from the center of rotation and has 1,5mm Al equivalent inherent filtration and additional compound filtration of 2mm Al and 0,1mm Cu. The tube potentials ranged from 40kVp to 130kVp. Exposures are pulsed and range from 0,1mAs to 500 mAs per X-ray projection. In the site opposite to the tube is located the amorphous silicon (AmSi) flat panel, which has an active area of 409,6x409,6mm and is located 536mm from the axis rotation.

CTDI measurements

CTDI measurements were performed in a phantom (Fluke Biomedical Model 76-414-4150) made of solid acrylic having a thickness of 15 cm and a diameter of 32 cm, in order to simulate the pelvis, or 16 cm, to simulate the head (Figure 1).These two phantoms contained five probe holes, one in the center and four around the perimeter, 90º apart from the center and 1cm from the edge. Each part includes five acrylic rods for plugging all the holes in the phantom. A 0,125cm^3 ionization chamber (TM3009, PTW Freiburg) was used in this study (Nk= 8,342*10^6 Gy/C and Kq=1.0 were introduced in PTW webline electrometer).

Measurements were made in the center and at four equal peripheral holes. For the pelvis, dose indices were acquired with 660 frames in full rotation (360º). The reconstructed diameter for this location was the medium field of view (FOV), corresponding to 410 mm. For the head, 361 frames were acquired with a 160º rotation and a small FOV, with 270 mm of diameter. In order to simulate the treatment setup for this location, the flat panel was shifted laterally to a corresponding asymmetric collimator.

The Report of the AAPM Task Group 75 recommends $CTDI_w$ to be a weighted index, since it reflects the weighted average of dose deposition in the peripheral (*p*) and centrer (*c*) as in the relation (1):

(1) $$CTDI_w = \frac{1}{3} CTDI_P + \frac{2}{3} CTDI_C$$, in mGy.

Figure 1: CTDI measurements for pelvis region (on the left) and Head region (on the right).

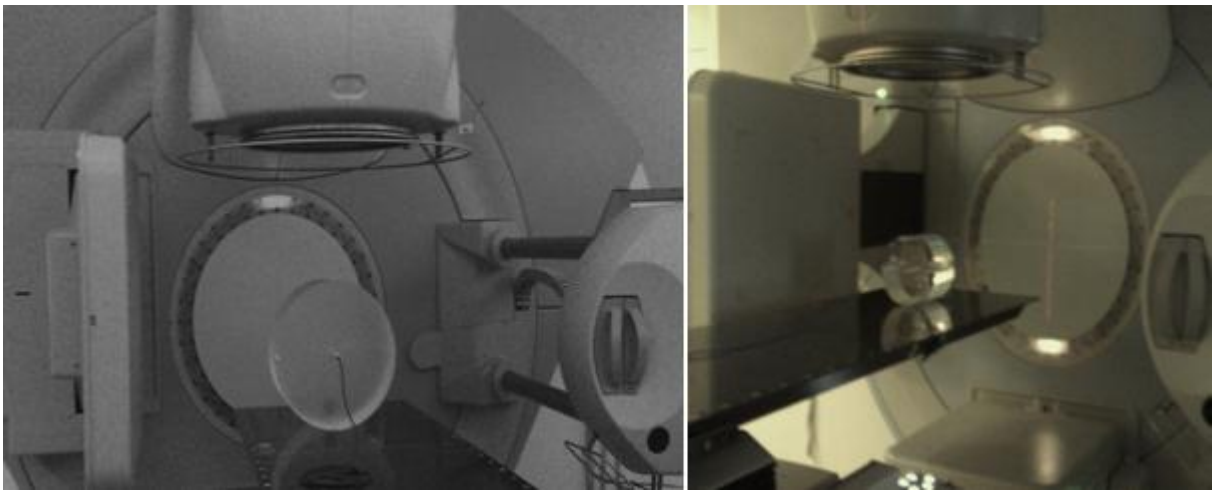

Patients

Prostate and HN patients were randomly selected. This study included 14 prostate patients and 7 HN patients. Regardless of the treatment technique, all patients underwent an IGRT protocol for verification of patient setup and treatment delivery conditions. All patients had localized tumours, with no known metastases in other organs. The HN patients were diagnosed with tumours located in the tongue (n=2), in the oral cavity (n=2), in the glottis (n=1), in the parotid (n=1) and in the cheek mucosa (n=1).

Prostate patients were instructed to urinate and drink 250mL of water 30 minutes before treatment. They were also told to empty their rectums 2 hours prior to each radiotherapy fraction. Nutritional support was provided, in order to allow for a diet without residue.

All patients signed an informed consent.

IGRT Protocol

Each imagiologic verification comprised of an acquisition before treatment. A post-correction acquisition was carried out to confirm SetD corrections.

The periodicity of acquisitions was consecutive for the first four fractions of treatment. A mean of the deviations from the three initial fractions was calculated, with the purpose of minimising systematic error and, thereafter, applied to the fourth treatment fraction. Weekly verifications were subsequently scheduled.

Deviation corrections were performed according to the defined tolerance values (TL), which were 3 mm for HN in all axes and for all treatment phases. For the first phase of treatment of the prostate group, tolerance values were 5 mm in the latero-medial (LM) and in the cranio-caudal (CC) axes, with 3 mm in the antero-posterior axis (AP). For the second and third treatment phases, tolerance values were defined, for the latter group, as 3 mm in all directions.

Setup deviation impact

In order to select the patients whose SetD were out of statistical control and to evaluate process quality, control charts were constructed for the mean and standard deviations of the setup deviations observed in the LM, CC and AP axes. The upper and lower control limits (UCL and LCL, respectively) were built with the values of 3 standard deviations and TL, which were previously described.

Patients with SetD out of the action limits and/or the TL on the control charts were selected from the sample of 21 patients. The analysis of the points in the control charts was restricted to points over or overlapping the control limits for mean and standard deviation (SD), since the established order of these points corresponds to each patient and not to a temporal observation.

For evaluating the SetD impact dose distribution a method described by Takemura et al.[25] was adapted. Initial dose distributions (dose distribution 1), approved at the beginning of treatment, were copied for the selected patients and new dose distributions (dose distribution 2) were carried out on the XIO® (CMS) TPS. The only difference applied to these new plannimetries was the isocenter location, in order to simulate SetD.

For SetD simulation, treatment fields were copied. As an example, if we consider 3 corrected SetD and an implemented mean of the systematic error for the ensuing fractions of HN treatment, prescribed as 2 Gy in 25 fractions, the initially generated fields were copied 4 times (the fields with the isocenter of the mean were prescribed with 22 fractions and the other 3 groups of fields with one fraction, corresponding to 3 corrected SetD). If SetD weren't corrected during the 3 initial fractions, the mean was applied to all the subsequent fractions. In order to find the new isocenter that took the corrected SetD or mean into account, a sum of the SetD values was calculated and applied to the number of fractions in which they occurred. After this, monitor unit number was verified and adjusted, if necessary, to be exactly equal to the dosimetric distribution 1. Normalization points were also maintained.

However, it became clear that the Multi Leaf Collimator (MLC) conformation was altered in the treatment planning system, when the isocenter coordinates were modified. In order to tackle this problem, the coordinates of each leaf pair was manually introduced for each field as to ensure that they would be in the exact same position of the initial plan.

Lastly, dose-volume histograms (DVH) were generated and the differences in dose received by organs at risk (OAR) were calculated between dose distribution 2 and dose distribution 1. The expression (2) summarizes what has been here described.

(2) $$Dif_{OAR} = x_{OAR2} - x_{OAR1}$$

Where Dif_{OAR} is the difference in dose, received by OAR (in percentage, %, of irradiated volume for prostate patients and in cGy for HN patients since for these mean and maximum doses were evaluated), x_{OAR2} is the OAR irradiated volume in dose distribution 2 (in % of irradiated volume, for prostate patients or cGy, for HN patients) and x_{OAR1} is the OAR irradiated volume in dose distribution 1 (in % of irradiated volume or cGy).

Differences in the Planning Target Volume (PTV) coverage with 95% of the prescribed dose (in cc) between the dose distribution 1 and dose distribution 2 were, likewise, compared. The expression (3) describes this is:

(3) $$Dif_{PTV} = v_{PTV2} - v_{PTV1}$$

Dif_{PTV} is the difference in the volume of the PTV coverage with 95% (in cc), v_{PTV2} is the volume of PTV coverage with 95% of the prescribed dose in the dose distribution 2 (in cc) and v_{PTV1} is the volume of PTV coverage with 95% of the prescribed dose in the dose distribution 1 (in cc).

Since there were differences in the OAR considered for treatment planning in the HN group, maximum and mean doses (cGy) were compared in these patients only for the spinal cord, since this is an organ commonly considered for all patients. For prostate patients, dose differences for the OAR were evaluated for bladder and rectum according to the following constraints: 50% of the bladder volume should only receive up to 70 Gy and 50%, 25% and 5% of the rectal volume should be irradiated with no more than 60 Gy, 72 Gy and 74 Gy respectively. Differences between the final and initial dose distributions were calculated and the results were analyzed. Differences in the coverage of volumes irradiated with 95% of the dose were evaluated for both pathologies.

For the analysis of the difference of the dose distribution values, either for the PTV coverage with 95% of the prescribed dose or for the aforementioned OAR assessment, a Wilcoxon test for paired samples was used. Statistical significance was considered with $p<0,05$.

RESULTS

CTDI

Table 1 shows the values of CTDI, CTDI peripheral and $CTDI_w$. Measurements of $CTDI_w$ for beam settings in the pelvis were 28.33, 28.45 and 26.44 mGy for 410 mm medium FOV, for M15F0, M15F1 and M10F1, respectively. For head, $CTDI_w$ measurement was 1,02 mGy.

A total of 76 HN pre-treatment CBCT (range 9-13, mean 10,86 acquisitions/patient) and 17 HN post-correction CBCT were performed. For prostate patients, 138 pre-treatment CBCT

Table1. Collimator and Filter cassettes, site and beam settings, FOV dimension and peripheral CTDI and weighted doses estimated for the clinical protocols adopted.

Collimator Cassettes/ Filter Cassettes	Site (beam settings)	FOV (mm)	CTDI peripheral (mGy)	CTDIw (mGy)
M15F0	Pelvis (120 kV/ 1040mAs)	410 mm	34,1	28,33
M15F1	Pelvis (120kV/ 1664mAs)	410 mm	33,48	28,45
M10F1	Pelvis (120kV/ 1664mAs)	410 mm	31,07	26,44
S10 F0	Head (100kV/36,1mAs)	270 mm	1,1	1,02

(range 6-14, mean 9,86 acquisitions/patient) and 34 post-correction CBCT were undertaken. Consequently, the administered doses, considering the preset used for each treatment, ranged from 9,18mGy to 15,76mGy (mean 13,5mGy/patient) for HN and from 170,7mGy to 528,8mGy (mean 337mGy/patient).

Control Charts

Control charts for mean (fig. 2a, 2b and 2c) and SD (2d, 2e and 2f) are presented in figure 2 for the initial phase on prostate treatments (respectively, for the LM, CC and AP axes). It is hence observable in the control charts for the mean (fig. 2a and 2c) that the control limits are never exceeded with the exception of the CC axis (fig. 2b), as the mean of the SetD for patient 21 is out of statistical control. For the initial phase of prostate treatment, TL are never exceeded in any case.

By analyzing the charts for the SD of each patient in this phase, it is readily detectable that patients 2 and 16 are out of statistical control in the LM axis and that patients 2, 3 and 21 are also out of statistical control in the CC axis. However, control limits are never exceeded in the AP direction.

Figure 3 displays the control charts for mean (Fig. 3a, 3b and 3c) and SD (Fig. 3d, 3e and 3f) in the boost phase of prostate treatment. Through analysis of these graphics, it is detectable that patients 10 and 16 have means overlapping to the superior control limits, namely in the LM and CC axes. For the charts considering the mean, patient 19 was observed to be out of the inferior TL in the LM axis but, however, not out of the inferior control limit. There is also a patient that exceeds the inferior control limit and the CC TL. On the AP axis, the control limits

Figure 2: Control charts for prostate setup errors in the initial phase

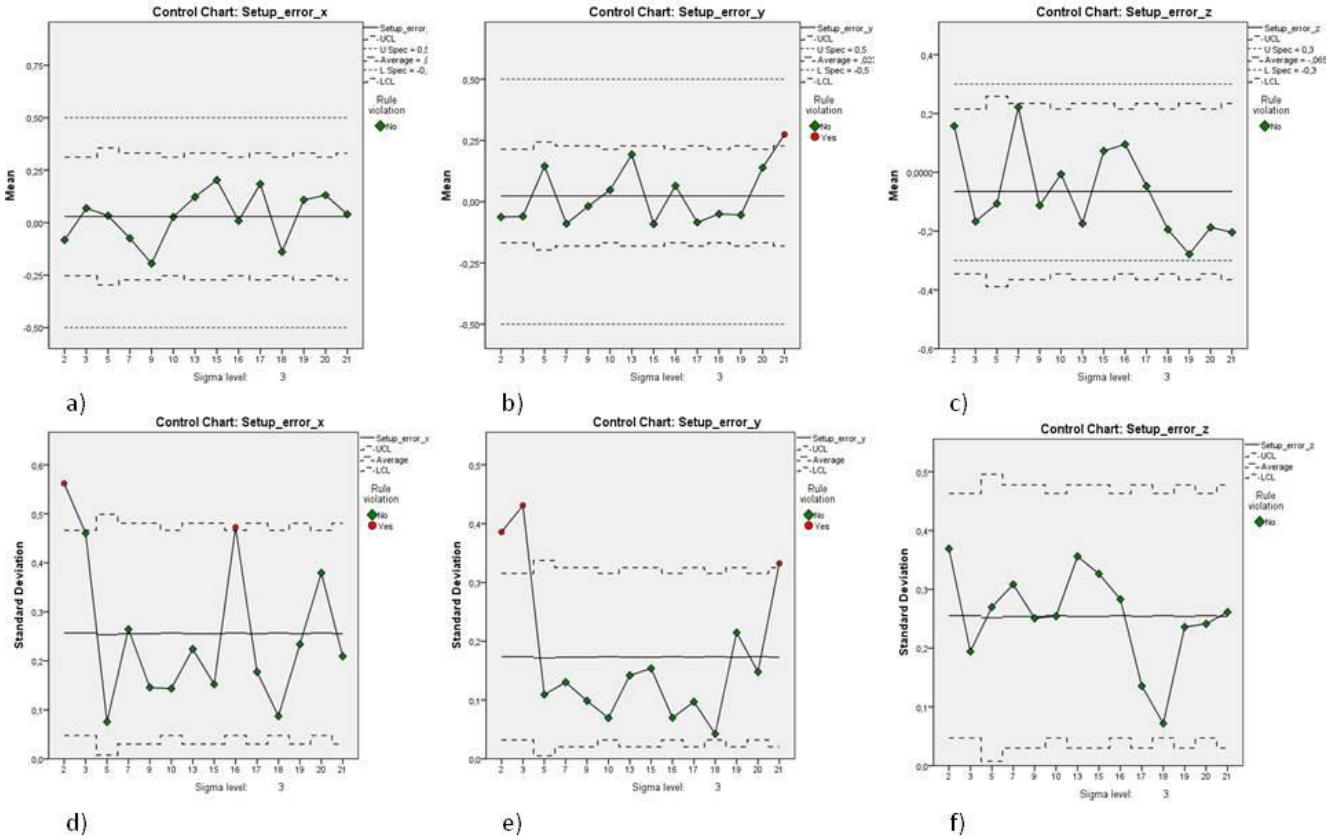

are never exceeded. Nevertheless, the superior TL is exceeded in the cases of patients 2, 3, 7 and 21. It is evident that patients 2 and 3 are out of control limits on the LM and CC axes, respectively, on the SD charts. On the AP axis, there are no patients that exceed the aforementioned control limits.

The control charts for the mean of the SetD of the initial phase in HN patients are displayed in figures 4a, 4b and 4c for the LM, CC and AP axes, respectively. It is observable that there are no points out of the control limits, except for the chart of the SetD in the AP axis, since the mean of the deviations in patient 12 is out of the inferior limit. After investigation of its causes, this discrepancy was attributed to the patient's severe weight loss, with increasing SetD during the first phase of treatment. In this case, during the last week of the initial phase, daily CBCT became mandatory. As a correction strategy during the boost phase, a new dosimetric planning was performed including obviously a new immobilization mask and a second planning CT. In the control charts of the SD on the LM (4d), CC (4e) and AP (4f) directions, patients 12, 6 and 1, respectively, had SD that exceeded the control limits.

Figure 3: Control charts for prostate setup errors in the boost phase

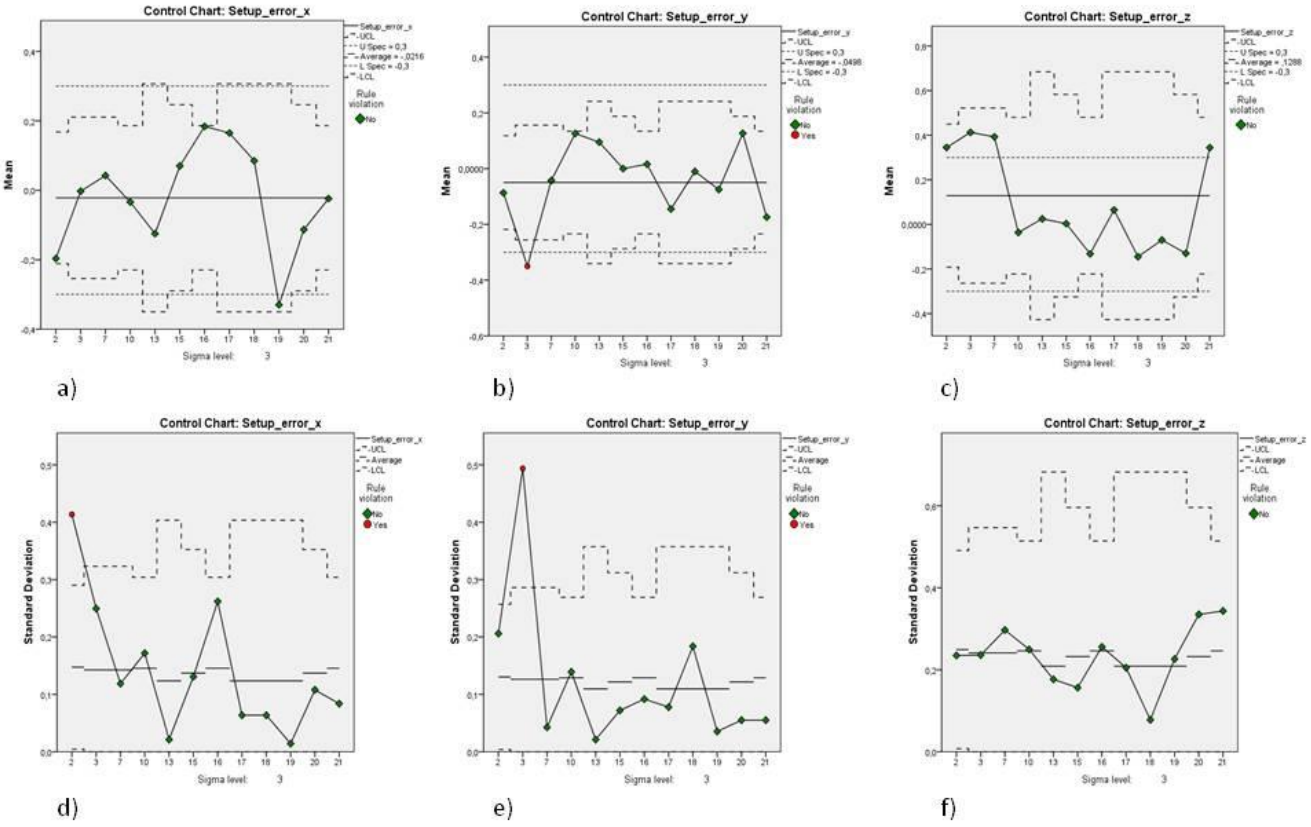

Through analyzing the control chart for the mean of the SetD during the boost phase (Fig. 5a, 5b and 5c) in HN patients, it can be observed that the SD of patients 4 and 11 is out of control limits in the AP and LM axes, respectively. Also worthy of note are the mean of patient 4, which is very close to the inferior control limit of the chart in the CC axis, and the mean of the SetD of patient 8, which exceeds the superior TL but keeps within control limits in the CC axis. In the control charts of the SD (Fig. 5d, 5e and 5f) there are no patients out of statistical control.

According to the results in the control charts, 6 prostate and 6 head and neck patients were selected for a new dosimetric distribution accounting for the setup errors on the isocenter position (distribution 2), with the intent of verifying what would have happened if these out-of-tolerance SetD had not been corrected. This was done by comparing distribution 2 to the dose distribution approved at the treatment planning phase (initial distribution or distribution 1), performed on the treatment planning computed tomography.

It is important to note that the patients out of statistical control were found not to comply with the dietary recommendations, even though they did not have a filled rectum as observed on CBCT imaging.

Figure 4: Control charts for HN setup errors in the initial phase

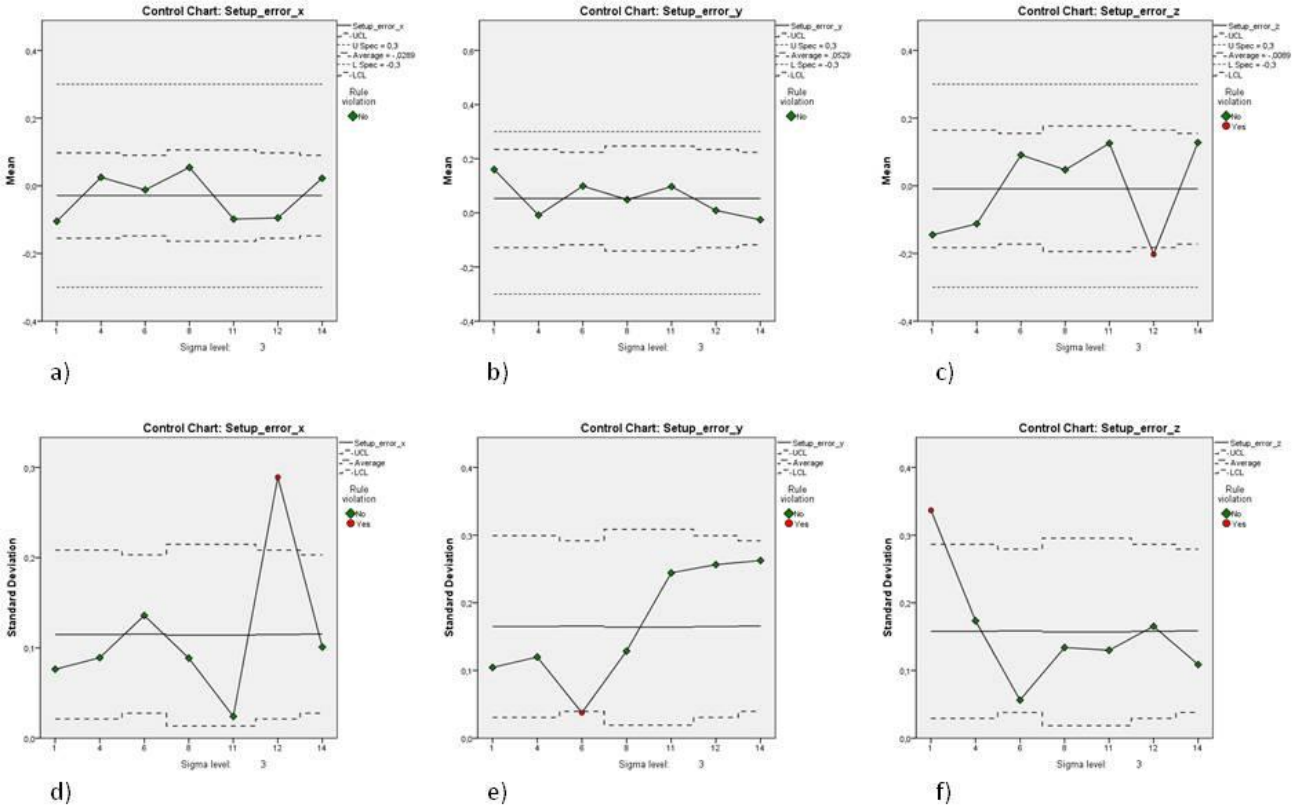

Dose distributions

Table 2 displays the result of Dif_{OAR} for the prostate patients. For this group, considered OAR were the rectum and the bladder and were evaluated according to aforementioned dose constraints. For patient 3, the prescribed dose was 65Gy, hence, bladder or rectal volumes irradiated with a dose equal or superior to 70Gy and 72Gy, respectively, were not considered. A negative value on the Dif_{OAR} reflects a decrease of the OAR irradiated volume in the dose distribution 2 which was performed with the observed setup errors, whereas a positive value represents an increase in the irradiated volume.

With the exception of patient 3, an increase in the difference of irradiated rectum corresponds to a decrease in bladder volume and vice-versa in all patients. Differences in dose distributions for the irradiated bladder volume percentage range from -4,69% to 5,44% (in average -1,4%).

It is noteworthy to state that, for 4 of the studied patients, a decrease of the bladder irradiated volume is observed in dose distribution 2, whereas an increase of bladder irradiated volume in dose distribution 2 happens in the other 2 patients. However, the bladder volume

Figure 5: Control charts for HN setup errors in the boost phase

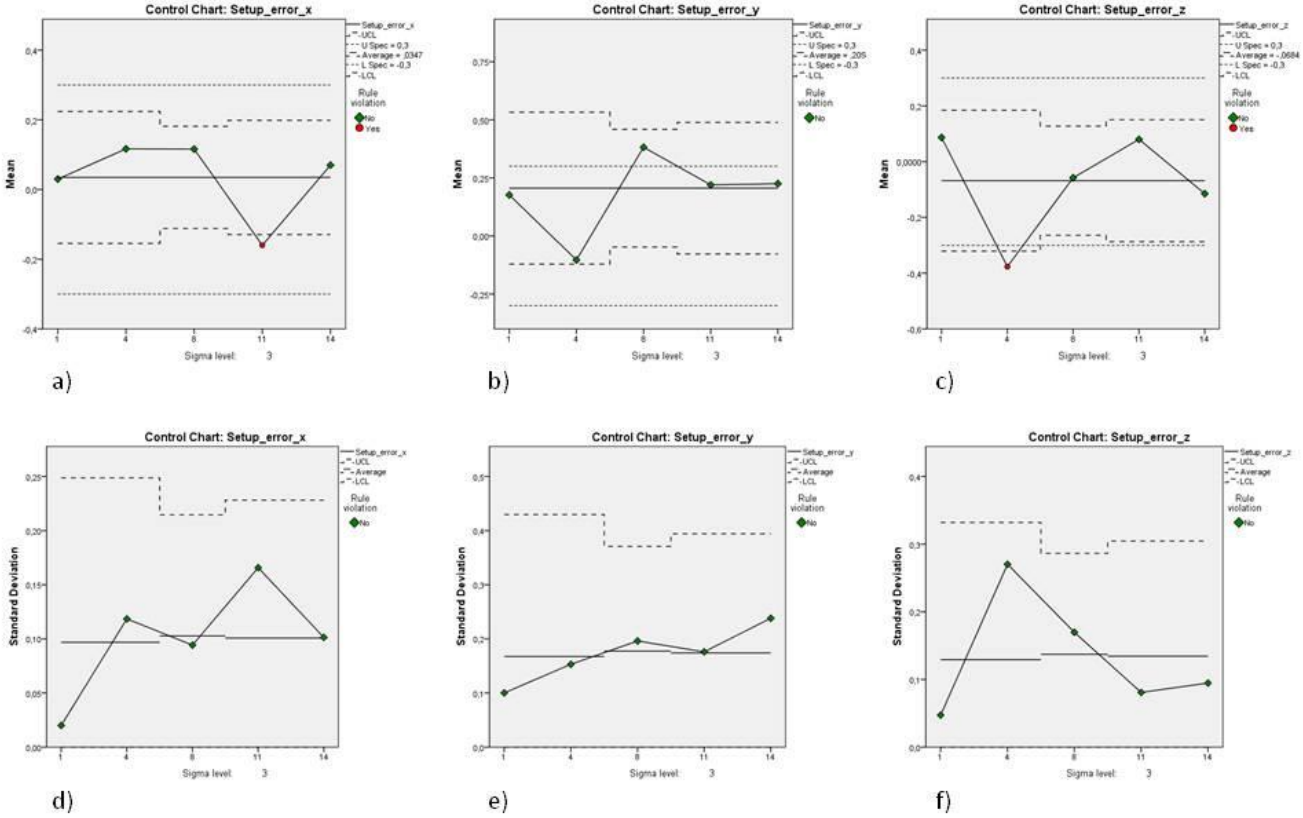

percentage irradiated with a dose equal or superior to 70Gy on distribution 2 does not significantly differ from the initial one (p=0,232).

Table 2. Difference in percentage of irradiated volume in bladder and rectum observed in the two dose distributions for prostate patients.

Dif_{OAR}, Differences in volume of organ at risk (% irradiated volume)				
Patient	Bladder ≥70Gy	Rectum ≥60 Gy	Rectum ≥72Gy	Rectum ≥74Gy
2	-3,97	9,81	1,61	0,26
3	NA	2,55	NA	NA
7	-4,6	14,83	16,38	11,29
10	1,22	-3,5	-1,72	-1,25
16	-4,69	6,62	4,46	3,47
19	5,44	-16,31	-12,48	-1,92
21	-1,83	9,75	7,78	6,29
Average, μ	-1,4	3,4	2,7	3

On the other hand, differences in dose distribution for the irradiated rectum volume ranged from -16,32% to 16,38% (in average 3,4, 2,7 and 3 for the Rectum≥60 Gy, 72Gy and 74Gy, respectively). In this case, it was verified that 5 of 7 patients had an increase of irradiated rectum volume for the measured dose constraints.

Nevertheless, the volume percentage of the irradiated rectal volume with a dose equal or superior to 60Gy, 72 Gy or 74 Gy on distribution 2 does not significantly differ from dose distribution 1 (p=0,199; p=0,232; p=0,232; respectively).

The difference in volume (cc) of the PTV (1; 2 and 3) irradiated with 95% of the prescribed dose between the dose distribution 2 and 1 is shown in Table 3. This was not evaluated in the case of the PTV3 of patient 3, since he did not have a third phase of treatment. The negative values displayed on the table reflect a decrease in this difference. These differences range from -40,3cc to 2,8cc for PTV1; -22,3cc to -4cc for PTV2 and -8,1cc to -2,7cc for PTV3.

Table 3. Dif_{PTV}, difference in PTV volume (cc) irradiated with 95% of the prescribed dose as observed in the two dose distributions for prostate patients.

Dif_{PTV}, Difference in irradiated PTV for prostate patients (in cc)			
Patient	PTV 1	PTV 2	PTV3
2	-11,37	-13,43	-5,19
3	-40,3	-22,3	NA
7	-14,1	-10,8	-4,4
10	-2,8	-6,6	-3,6
16	-4,8	-5,4	-4,1
19	-15,4	-11,7	-8,1
21	-4,4	-4	-2,7
Average, μ	-13,3	-10,6	-4,7

In all cases, distribution 2 demonstrates that there is a decrease in the volume irradiated with 95% of the prescribed dose against the initial distribution (dose distribution 1).

The median of the PTV1, PTV2 and PTV3 volumes irradiated with 95% of the prescribed dose for distribution 2 was significantly lower than on the initial distributions (p=0,009; p=0.009 and p=0,014; respectively).

Table 4 displays the result of the differences of the maximum and mean doses on the spinal cord of HN patients between dose distribution 1 and 2. As stated earlier in other instances, a negative value for these differences reflects a decrease in the dose as observed on distribution 2. This was, however, not performed in the case of patient 6, since the spinal cord was not considered as an organ at risk for the initial distribution.

Three of the analyzed patients would have an inferior dose maximum if the SetD had not been corrected, however, two patients have an increase in this dose maximum. It is also observable that the mean dose on the spinal cord would increase only in one patient and would diminish in 4 other cases if the SetD had not been corrected.

The median of the dose maximum on the spinal cord does not significantly differ between distributions 2 and 1(p=0,229). A similar observation was made for the median of the mean dose on the spinal cord (p=0,137).

Table 4. Difference in percentage of spinal cord maximum and mean observed in two dose distributions for HN patients.

Volume irradiated (in cc)		
Patient	Spinal cord max	Spinal cord mean
1	86	21
4	-103	-59
6	NA	NA
8	-36,8	-17,3
11	-66	-7
12	64	-33

The difference in volume (in cc) of both PTV1 and PTV2 irradiated with 95% of the prescribed dose between distribution 1 and 2 is presented on table 5. This difference was not assessed for patient 6, since in this case there was no second phase of treatment.

The negative values on this table report a decrease in the volume of the PTV irradiated with 95% of the prescribed dose between dose distribution 2 and 1, so a negative value implies that the volume covered with 95% of the dose was inferior in distribution 2.

As can be seen, differences in these values range from -7,4cc to 3,3cc for PTV1 and from -5,1cc to 0.8 cc for PTV2.

For PTV1, in all cases, distribution 2 demonstrates a decrease in the volume irradiated with 95% of the prescribed dose with the exception of patient 1. In the case of PTV2 results are similar, with a decrease in values for all patients except for patient 2, in whose case there is an increase in the volume of the PTV2 irradiated with 95% of the dose and for patient 12, for whom no difference can be noted.

The median of the volume of PTV1 irradiated with 95% of the prescribed dose on distribution 2 is significantly inferior to this value as verified on the initial distribution (p=0,0365). For the

PTV2, the median of the volume covered with 95% of the prescribed dose does not differ significantly between dose distributions (p=0,1425).

Table 5. Difference in cc, on PTV 1 and 2 observed in two dose distribution for HN patients.

Volume irradiated com 95% da dose prescrita (in cc)		
Patient	PTV 1	PTV 2
1	2,5	0,8
4	-3,4	-5,1
6	3,3	NA
8	-1,9	-2,2
11	-4,7	-0,9
12	-7,4	0
Average, μ	-1,9	-1,5

DISCUSSION:

The main purposes of the reported work were to quantify SetD during radiotherapy for prostate and head and neck (HN) pathologies, as measured with CBCT. Justification of CBCT doses administered to the patients was hence performed, verifying the eventual treatment benefit of this IGRT protocol by simulation of the SetD during radiotherapy in dose distributions. This allowed for predicting a situation in which these errors would not have been corrected. The adequacy of the imaging protocol for these pathologies was assessed. Finally, the identification of an optimal point between imaging dose and beam alignment error correction, which is a key issue in the precision of radiotherapy delivery, was also addressed. The TL for the initial prostate treatment phase, either for the mean or for the standard deviation, are never exceeded. This might result from the fact that every patient was carefully instructed about rectum and bladder preparation. It is noteworthy that the LM and CC TL set for the initial phase of the prostate should be rethought, since the mean values of the SetD of the sample set never exceed ± 0.3 cm. Patients were also instructed to repeat the preparation protocol again in case a rectal and/or bladder filling that differed from the planned one was observed on pre-treatment control imaging. Still it is important to state that the SD for the prostate patients was high, because even when the means of SetD are in control, most patients are out of statistical control in SD charts. This induced us to think about our methods and protocols.

The TL at the initial phase of HN treatment could also be reduced, since the mean of the SetD is never superior to ± 0,2 cm in the LM and CC directions. On the AP axis, the mean is always inferior to ±0,25cm.

In view of the results observed on the control charts, it is clear that 29% and 25% of the sample set of patients with prostate tumours is out of statistical control on the initial and boost phases of treatment, respectively. In the case of the HN group, 43% of the sample set is out of statistical control, however, in the boost phase, this proportion is reduced to 33%.

Through the simulation reported in this work, it was found that if the SetD had not been corrected, there would not be a significant difference on the median of the percentage of the irradiated volume of the OAR for prostate patients. Interestingly for PTV coverage with 95% of the prescribed dose, the opposite is observed, with a decrease of, in average 13,3 cc in PTV1, 10,6 cc in PTV2 and 4,7 cc in PTV3. This demonstrates a therapeutic gain through the use of verification imaging, even though we are increasing the delivered dose by 337 mGy (in average) with its use. This increment is obtained through ensuring that the planned dose is indeed administered on the target volume and that this volume is treated globally and reproducibly.

Regarding the HN patients, there was no significant difference in median values of the mean dose delivered to the spinal cord after comparison of the aforementioned dose distributions. Yet, there is a significant decrease in PTV1 coverage with 95% of the prescribed dose when comparison of the distribution 1 with distribution 2 was undertaken, with an average of -1,9 cc in loss. This difference was not observed for PTV2. It is thus clear that, from the therapeutic perspective, there is an increase in the therapeutic ratio from the increment of dose delivery of an average of 13,5 mGy/patient provoked by verification imaging, since the tumour control probability might again be affected by a decreased dose coverage of the target volume.

Other positive aspects might be inferred from the reported observations, since the visualization of target volumes and surrounding structures allow for monitoring of the filling status of organs such as the bladder or the rectum. It is also possible to assess the status of the target volume itself, which might decrease, move and thus be altered during treatment.

CONCLUSION:

Even though this is a small series of patients, the reported work clearly states both the utility and feasibility of the IGRT protocol in view of the dose-benefit paradigm, with a solid justification of the dose increment delivery through the use of the CBCT imaging tool. Indeed, simulated data confirmed the point of using CBCT according to the described protocol.

In the future, studies should be made to allow for the CBCT dose to be accounted for in the treatment planning phase, even though there are difficulties in adding this dose to the prescribed one, as described by Murphy et al. [21]

This work allowed for determination of aspects of our IGRT protocol that need to be rethought, namely on the TL. These must be chiefly re-assessed in the LM and CC axes during the first phase of treatment for prostate tumours, whereas for HN tumours this must be done for all axes.

To conclude, the next steps in the adaptation of the IGRT protocol will be to study and recalculate the TL, just as defining the correct methodology to apply these in all cases. In the ever developing field of radiotherapy precision, adapting and revising these protocols, in light of new imaging tools, will bring clear gains in the treatment of patients with such a devastating disease as cancer proves to be.

Acknowledgments: The authors want to thank to Luis Madureira, Ana Duarte and Ana Rato for helping us with CTDI acquisitions and dose distribution analyses.

References:

1. Verellen D., Ridder M., Tournel K., Duchateau M., Reynders T., Gevaert T., Linthout N., Storme g. An overview of volumetric imaging technologies and their quality assurance for IGRT. Acta Oncol 2008,47:1271-1278.

2. Verellen D, Ridder M, Storme G. A (short) history of image-guided radiotherapy. Radiother Oncol 2008;86:4–13.

3. Xing L., Thorndyke B., Schreibmann E., Yang Y., Li T., Kim G., Luxton G., Koong A. Overview of image-guided Radiation Therapy. Med Dosim 2006;31:91-112.

4. Olsen D., Thwaites D. Now you see it…Imaging in radiotherapy treatment planning and delivery. Radiother Oncol 2007;85:173-175

5. Van Herk M. Errors and Margins in Radiotherapy. Seminars Radiat Oncol 2004 January;14, (1):52-64.

6. Van Herk M, Remeijer P, Rasch C, Lebesque J. The Probability of correct target dosage: Dose-population histograms for deriving treatment margins in Radiotherapy. Int J Radiat Oncol Biol Phys 2000;47(4):1121–1135.

7. Langen K, Jones T. Organ Motion and its Management. Int J Radiat Oncol Biol. Phys 2001;50(1):265–278.

8. Yan D, Lockman D, Martinez A, Wong J, Brabbins D, Vicini F, Liang J, Kestin L. Computed Tomography Guided Management of Interfractional Patient Variation. Semin Radiat Oncol 2005;15:168-179.

9. The Royal College of Radiologists, Society and College of Radiographers, Institute of Physics and Engineering in Medicine. On Target: ensuring geometric accuracy in Radiotherapy. London: The Royal College of Radiologist, 2008.
10. Korreman S, Rasch C, McNair H, Verellen D, Oelfke U, Maingon P, Mijnheer B, Khoo V. The European Society of Therapeutic Radiology and Oncology–European Institute of Radiotherapy (ESTRO–EIR) report on 3D CT-based in-room image guidance systems: A practical and technical review and guide. Radiother Oncol 2010;94:129–144.
11. Van Herk M, Different styles of Image-Guided Radiotherapy. Semin Radiat Oncol 2007; 17:258-267.
12. Dawson L, Sharpe M. Image-guided radiotherapy: rationale, benefi ts, and Limitations. Lancet Oncol 2006;7:848–58
13. Yan D and Lockman D. Organ/patient geometric variation in external beam radiotherapy and its effects. Med Phys 2001;28(4):593-602
14. Kupelian P., Langen K., Willoughby T., Zeidan O., Meeks S. Image-Guided Radiotherapy for Localized Prostate Cancer: Treating a Moving Target. Semin Radiat Oncol 2008;18:58-66.
15. Huang E., Dong L., Chandra A., Kuban D., Rosen I., Evans A., Pollack A. Intrafraction prostate motion during IMRT for Prostate Cancer. Int J Radiat Oncol Biol Phys 2002;53(2):261–268.
16. Xu F., Wang J., Bai S., Xu Q., Shen Y., Zhong R. Interfractional and intrafractional setup errors in radiotherapy for tumors analyzed by cone-beam computed tomography. Chin J Cancer 2008;27(10):372-376.
17. Xu F., Wang J., Bai S., Li Y., Shen Y., Zhong R., Jiang X., Xu Q. Detection of intrafractional tumour position error in radiotherapy utilizing cone beam computed tomography. Radiother and Oncol 2009;89:311–319.
18. Wang J., Bai S., Chen N., Xu F., Jiang X., Li Y., Xu Q., Shen Y., Zhang H., Gong Y., Zhong R., Jiang Q. The clinical feasibility and effect of online cone beam computer tomography-guided intensity-modulated radiotherapy for nasopharyngeal cancer. Radiother and Oncol 2009;90:221–227.
19. Smitsmans M., Pos F, Bois J., Heemsbergen W., Sonke J., Lesbesque J., Van Herk M. The influence of a dietary protocol on Cone Beam CT-Guided Radiotherapy For Prostate Cancer Patients. Int J Radiat Oncol Biol Phys 2008;71(4):1279–1286.
20. Létourneau D, Martinez AA, Lockman D, Yan D, Vargas C, Ivaldi G, Wong J. Assessment of residual error for online cone-beam CT-guided treatment of prostate cancer patients. Int J Radiat Oncol Biol Phys 2005;62(4):1239–1246.

21. Murphy M, Balter J, Balter S, BenComo J, Das I, Jiang S, Ma C, Olivera G, Rodebaugh R, Ruchala K, Shirato H, Yin F. The management of imaging dose during image-guided radiotherapy: Report of the AAPM task Group 75. Med Phys 2007;34(10):4041-4063.
22. Amer A, Marchant T, Sykes J, Czajka J, Moore C. Imaging doses from the Elekta Synergy X-ray cone beam CT system. Br J Radiol 2007;80:476–482.
23. Islam M., Purdie T.,Norrlinger B., Alasti H., Moseley D., Sharpe M., Siewerdsen J, Jaffray D. Patient dose from kilovoltage cone beam computed tomography imaging in radiation therapy Med Phys 2006;33(6):1572-82.
24. Walter C., Boda-Heggemann J., Wertz H., Loeb J, Rahn A.,Lohr F.,Wenz F. Phantom and in-vivo measurements of dose exposure by image-guided radiotherapy (IGRT): MV portal images vs. Kv portal images vs. cone-beam CT. Radiot Oncol 2007;85:418–423.
25. Takemura A, Shoji S, Ueda S, Kurata Y, Kumano T, Takamatsu S, Suzuki M. Effect of daily setup errors on individual dose distribution in conventional radiotherapy: an initial study. Radiot Phys Tecnhol 2009;2(2):151-8.

IMPACT OF RANDOM AND SYSTEMATIC ERRORS IN THE DAILY PRACTICE IN RADIOTHERAPY

ANA RITA SIMÕES[1], MARGARIDA EIRAS[2], ISABEL MONTEIRO GRILLO[1].

1-SERVIÇO DE RADIOTERAPIA, HOSPITAL DE SANTA MARIA, CENTRO HOSPITALAR LISBOA NORTE, EPE.
2-ESCOLA SUPERIOR DE TECNOLOGIA DA SAÚDE DE LISBOA.

ABSTRACT:

BACKGROUND/PURPOSE: Radiotherapy precision is an important issue in current state of the art treatment methods. In order to ensure target volume coverage and organs at risk sparing, ensuring that radiation is delivered to intended targets is of utmost importance. Image-guided radiotherapy (IGRT) provides us with useful tools to address this problem. However, in order to allow for correct use of these technologies and ensuring proper treatment delivery methods, systematic and random errors need to be assessed and accounted for at the treatment planning and delivery stages.

MATERIAL/METHODS: 21 patients (pts) undergoing prostate or head and neck (HN) radiotherapy at our department were randomly selected and underwent an IGRT protocol resorting to cone-beam computed tomography (CBCT) as the verification imaging technique. Setup error analysis was performed in order to evaluate systematic and random errors during treatment delivery in the cranio-caudal (CC), latero-medial (LM) and antero-posterior (AP) directions.

RESULTS: Intrafraction movements do not increase during HN treatment except for the LM direction. In the case of the prostate group, the most increased systematic error values are observed in the AP direction. For the initial phase of HN treatment, ideal margins for PTV are 2,1mm, 3,5mm and 2,1mm, in the LM, CC and AP directions respectively. For the boost phase, values thus calculated are 4,0 mm, 1,6 mm e 2,7 mm in the same order. In the prostate group, ideal margins of 4,8mm, 4,3mm and 5,4mm for the initial phase in the LM, CC and AP axes were calculated, whereas for the boost phase 5,7mm, 6,5mm e 8,0mm margins were obtained, considering the same order.

CONCLUSIONS: Patient information on dietary requirements, rectal and bladder preparation should be stressed and informative methods revised. PTV margins used at our department

might be reduced for both phases of HN cancer treatment and for the initial prostate cancer treatment phase. However, margins applied at the treatment planning stage in the prostate boost phase need to be increased.

Keywords: Setup Errors, Sistematic Error, Random Error and Isotropic Margins

INTRODUCTION

Precision is a key issue in current state of the art radiotherapy. In fact, as we moved from 2D to 3D imaging techniques and with the subsequent application of more refined radiotherapy technologies, such as Intensity Modulated Radiotherapy (IMRT) or stereotactic radiotherapy, ascertaining that radiation is delivered to the intended targets has become more important than ever. Indeed, radiation accuracy is logically coupled to an increase in tumour control probability and a concurrent decrease in treatment-related toxicity. However, the advent of such concepts, with a close conformity to the tumour progressively becoming the paradigm in this cancer treatment method, imposes treatment accuracy as a crucial aspect of modern radiotherapy. [1]

The ever evolving field of image-guided Radiotherapy (IGRT) provides us with the tools for bringing this important issue to new harbours. Indeed, this has been the focus of active research and development in recent years, with exciting new technologies being looked into and applied in numerous centers around the globe. One of these advents was the Cone Beam Computed Tomography (CBCT), which allowed us to perform computed tomography (CT) immediately before radiotherapy fractions.[2-6] Thus, we are nowadays empowered with the means to compare, with nearly identical resources, patient data, obtained at the planning and treatment delivery stages, in a safe and effective way. This might allow us to reduce margins used for treatment planning, with a consequent decrease in toxicity, but still keeping treated volumes focused on the tumour and any of its microscopic extensions.[7]

However, we still rely on guidelines yielded by key, world-class, institutes of reference. Although these guidelines provide crucial information that enables other departments to implement techniques in a somewhat faster way, it is important to study the impact of these new radiotherapy delivery methods, in order to provide patients with quality-assured and reliable treatments.[8] Furthermore, people and technology differ between departments and guidelines implemented in a particular case might help, but they cannot replace data obtained locally, in the actual working conditions of a particular healthcare unit.

The work hereby reported focused on quantifying the translational and rotational setup deviations, as well as quantifying the intrafraction movements and setup errors in head and neck (HN) and prostate cancer patients treated at our department. Its main purpose is,

therefore, to adapt our currently implemented IGRT protocol in light of this data. In order to tackle these issues, rotational and translational deviations were quantified for prostate and HN patients during treatment, resorting to CBCT as a way to detect differences during radiotherapy. In addition, the question of the direction with the most important amplitude of deviation is addressed, as is the eventual difference in systematic and random errors between the initial and boost phases, since these subjects might yield new paradigms at the radiotherapy planning stage.

METHODS AND MATERIALS

Patients

From May 2011 to September 2011, patients with prostate and HN cancer undergoing radiotherapy at our department were randomly selected. This study included 21 patients, 19 male and 2 female, with a mean age of 65 (range 36-79) years. Diagnoses were prostate cancer in 14 cases and HN cancer in the remaining 7 cases. For the HN patients, 2 were diagnosed with tumours of the tongue, 2 with oral cavity cancer and the remainder 3 cases had a diagnosis of glottis, parotid and cheek mucosa tumours. All prostate patients had an adenocarcinoma histology and all the HN patients had squamous cell carcinomas, except for the parotid case, in which an adenocarcinoma was confirmed. All the patients had localized tumours, with no clinical evidence of distant metastases. They all had Karnofsky indices that were superior to 70%.

Regardless of the treatment technique, all patients underwent an IGRT protocol for verification of patient setup and treatment delivery conditions.

All patients signed an informed consent.

Patient Positioning

All HN patients were set in a supine position, with their arms along the body, with both palmar regions touching the table. The MedTech™ (CVICO®) head and shoulder mask fixation system, as well as thermoplastic head and shoulder masks were used in HN patients, in order to immobilize the HN region during planning CT and all treatment sessions. A planning CT with 3mm slices was performed from the vertex of the skull to 3 cm bellow the xiphoid process.

Prostate patients were set in a supine position using the Combi-Fix™ (CVICO®) baseplate, which combines feet and knee support. Planning CT was acquired from the fourth lumbar vertebra to 3 cm below the tuberosity of the ischium. For these patients, a bladder and rectum preparation was recommended: patients were asked to urinate and drink 250 mL of

water 30 minutes before treatment and planning CT and instructed to empty their rectums 2 to 3 hours prior to treatment and planning CT. All patients underwent a dietary protocol in order to minimize bowel movements.

CBCT scans and IGRT Protocol

For each HN patient, CBCT was obtained with 100 kV, 361 mAs, 205º of gantry rotation, acquiring 361 frames. The prostate parameters for CBCT imaging were 120 kV, 1040 mAs, 360º of gantry rotation and 650 frames were acquired.

All setup errors were analyzed with the Elekta X-ray Volume image (XVI) software. Automatic-3D registration of the reference planning CT and CBCT scans was performed using the cross-relation algorithm provided in this Elekta software. In order to obtain setup errors, CBCT images were acquired according to our IGRT protocol, as described below. An automatic grey-value matching was performed for prostate patients and an automatic bone matching was obtained for HN patients. The HN alignment clip-box was defined to include all the PTV and surrounding bones, like vertebras and the base of skull, excluding chin. The prostate alignment clip-box was defined to include the whole PTV, surrounding tissues like the bladder and bones, such as the femoral heads. The rectal volume was excluded to the maximum possible extent.

In order to assess patient positioning, a pre-treatment (pre-tt) CBCT acquisition was executed for all imaging verifications. A post-treatment (post-tt) acquisition was also obtained to evaluate treatment reproducibility. For every setup error correction, a post-correction acquisition was performed in order to confirm accurate positioning.

The timing of acquisition was consecutive for the first four treatment fractions. An average of the setup errors was calculated for the first three fractions to allow for systematic error minimization and applied at the fourth fraction of treatment. Subsequently, verifications were scheduled on a weekly basis.

During weekly verification, only setup errors were corrected, according to defined values. These were 3 mm for HN in all axes and for all treatment phases. For the prostate group, an action level (AL) values were defined for the first phase of treatment as 5 mm in the latero-medial (LM) and cranio-caudal (CC) axes; 3 mm were defined in the antero-posterior (AP) direction. For the second and third treatment phases in the latter group, AL was defined as 3 mm in all axes.

Table 1. HN Translational setup errors for the initial and boost phases of treatment.

HN translational setup errors										
		M (mm)			∑ (mm)			σ (mm)		
		LM	CC	AP	LM	CC	AP	LM	CC	AP
First treatment Phase	Pre-treatment (N=56)	-0,3	0,5	-0,1	1,2	1,0	1,8	0,8	1,5	1,1
	Post-correction (N=9)	0,3	0,5	-0,2	0,4	0,3	0,1	1,0	0,4	1,3
	Post-treatment (N=51)	-0,4	0,0	-0,7	0,4	0,7	1,6	1,3	1,1	1,3
Boost treatment phase	Pre-treatment (N=20)	0,4	1,8	-0,9	1,7	1,8	2,2	0,9	1,1	1,0
	Post-correction (N=8)	0,3	-0,2	-1,1	1,1	1,1	1,1	0,4	0,5	0,5
	Post-treatment (N=17)	0,1	0,4	-0,6	0,6	1,4	1,3	0,8	0,7	0,2

XVI quality assurance was carried out monthly by checking geometric accuracy, image quality and safety of the mechanical system.

Setup error analysis

Initially, the mean and standard deviation were calculated, for each patient. The group mean (M) is the mean of all means. The systematic error (∑) of setup positioning was defined as the variability of the mean and was calculated as the standard deviation of the individual means. The random error (σ) was defined as the root-mean-square of the individual standard deviation of setup error in each patient.[9] Intrafraction movement was also calculated for both groups as the difference between the post-tt and pre-tt acquisitions. The Wilcoxon signed-rank test was used to assess the differences in the pre-tt and post-tt translational and rotational setup errors. In order to assess intrafraction movement, a Mann-Whitney test was used to compare the means in the three axes. The Kruskal-Wallis one-way analysis of variance was used to test the differences in intrafraction movement during treatment. Statistical significance was considered when the p value was inferior to 0,05.

RESULTS

Twenty-one patients underwent CBCT scan for 7-17 fractions of their treatment, with a mean of 11 CBCT for HN patients and 10 CBCT for prostate patients. A total of 161 HN CBCT and 294 prostate CBCT were acquired, including 214 pre-treatment CBCT in both pathologies, 51 pre-correction CBCT and 190 post-treatment CBCT.

Table 2. HN rotational setup errors for the initial and boost phases of treatment.

HN rotational setup errors										
		M (º)			∑ (º)			σ (º)		
		LM	CC	AP	LM	CC	AP	LM	CC	AP
First treatment Phase	Pre-treatment (N=56)	1,1	-2,6	0,4	0,6	5,3	0,6	0,4	3,0	0,3
	Post-correction (N=9)	1,2	0,1	0,5	1,0	0,3	0,3	0,6	0,8	0,7
	Post-treatment (N=51)	1,0	-0,4	0,4	0,8	0,7	0,4	0,5	0,5	0,4
Boost treatment phase	Pre-treatment (N=20)	0,8	0,2	0,1	1,4	0,3	0,8	0,4	0,8	0,5
	Post-correction (N=8)	0,2	0,3	0,0	1,1	1,0	0,7	1,4	0,5	0,2
	Post-treatment (N=17)	0,7	0,2	0,2	1,1	0,7	1,1	0,1	0,5	0,6

Tables 1 and 2 summarize the translational and rotational setup errors, respectively. As can be observed, the M of the translational setup errors of the first phase of treatment is ranged between -0,7 and 0,5 mm, the range of ∑ is from 0,1 to 1,8 mm and the σ is ranged from 0,8 to 1,3 mm. For the boost phase, a marked difference is observed, since the calculated M ranges from -1,1 to 1,8 mm and the ∑ is ranged from 0,6 to 2,2 mm. In this case, σ ranged from 0,2 to 1,1 mm. It is noteworthy that, for the initial phase of treatment, 72,1% of the pre-tt translational deviations on the LM direction in HN patients range from -2 to 2 mm. The same range is observed for 71,1% of the setup errors in the CC and for 67,3% in the AP axis. For the boost phase, this observation is also valid for 85% of the setup errors in the LM, for 45% in the CC and for 80% in the AP directions.

For the initial phase of treatment, the M of the measured rotational setup errors is ranged from -2,6º e 1,1º, ∑ ranges from 0,3º to 5,3º and σ ranges between 0,1º and 1,4º. For the boost phase the interval of M ranges from 0º a 0,8º, ∑ ranges from 0,3º to 1,4º and σ ranges from 0,1º to 1,4º.

The median of the post-tt translational setup errors is therefore superior to the median of the pre-tt setup errors in all axes, with the exception of the AP direction. (p value=0,0235 for the LM direction, p value= 0,0025 for the CC direction and p value= 0,3525 for AP direction). No significant difference in the rotational deviations was found when compared to the pre-tt setup errors.

It was also observed that, in the case of intrafraction movement in these pathologies, there is a significant increase in the LM axis (p= 0,043), however, this is not observed for the other two axes, in which there is no significant difference.

Table 3. Prostate translational setup errors for the initial and boost phases of treatment.

Prostate translation error										
		M (mm)			∑ (mm)			σ (mm)		
		LM	CC	AP	LM	CC	AP	LM	CC	AP
First treatment Phase	Pre-treatment (N=99)	0,3	0,2	-0,7	1,1	1,2	1,5	2,8	2,0	2,5
	Post-correction (N=27)	0,3	-0,1	-0,2	0,5	0,4	0,8	0,9	0,4	0,6
	Post-treatment (N=88)	0,0	0,1	-0,6	1,3	0,8	0,7	1,3	1,4	1,4
Boost treatment phase	Pre-treatment (N=39)	-0,2	-0,5	1,3	1,9	2,0	2,9	1,4	2,0	1,2
	Post-correction (N=7)	-0,1	-0,1	-0,4	0,6	0,4	0,7	0,6	0,4	0,4
	Post-treatment (N=34)	-0,3	0,2	-0,2	1,2	1,0	0,8	1,0	0,3	0,4

Significant differences in the intrafraction movement were not observed during treatment for LM and CC direction (p= 0,146 and 0,1295, respectively). However it was found that intrafraction movement increases in the course of treatment for the AP axis (p=0,0265). The translational and rotational setup errors for the prostate groups are displayed on tables 3 and 4, respectively. For the initial phase of treatment, M is ranged between -0,7 and 0,3 mm, ∑ between 0,4 and 1,5 mm and σ ranges from 0,4 to 2,8 mm. For the boost phase, M ranges from -0,2 to 1,3 mm, ∑ from 0,4 to 2,9 mm and σ ranges from 0,3 to 2,0
mm. On the translational pre-tt setup errors in the LM direction in prostate patients, 82,8% of these are ranged between -3,5 and 3,5 mm; the same is observed for 88,4% of these in the 90,6% of the pre-tt setup errors in the LM axis, for 95,3% in the CC axis and for 67,4% in the CC and 76,7% in the AP directions. In the boost phase, the same range was for the AP axis.
No significant difference in the translational deviations was found when compared to the pre-tt setup errors and for rotational CC axis deviations. However, an increase in post-tt deviations was noted for the LM and AP directions, when compared to pre-tt data (p value= 0,002 and 0,0 respectively).
For the initial phase of treatment, the M of the measured rotational setup errors is ranged from -0,1º e 0,4º, ∑ ranged from 0,4º to 1,5º and σ ranges between 0,2º and 1º. For the boost phase the interval of M ranges from -0,3º a 0,6º, ∑ ranges from 0,4º to 1,6º and σ ranges from 0,0º to 1,1º.
No significant differences were observed for the mean of the intrafraction movements, which were not demonstrated to increase during treatment of prostate cancer patients.

Table 4. Prostate Rotational setup errors for the initial and boost phases of treatment.

		Prostate Rotational error								
		M (mm)			∑ (mm)			σ (mm)		
		LM	CC	AP	LM	CC	AP	LM	CC	AP
First treatment phase	Pre-treatment (N=99)	0,1	0,1	-0,1	1,4	0,5	0,4	0,6	0,2	0,2
	Post-correction (N=27)	0,1	0,2	-0,1	1,5	0,7	0,4	0,9	0,5	0,2
	Post-treatment (N=88)	0,4	0,2	0,0	1,1	0,7	0,5	1,0	0,2	0,2
Boost treatment phase	Pre-treatment (N=39)	0,4	0,1	-0,1	1,5	0,6	0,4	1,0	0,6	0,3
	Post-correction (N=7)	-0,2	0,1	-0,3	1,6	0,5	0,5	1,1	0,3	0,0
	Post-treatment (N=34)	0,6	0,3	-0,1	1,3	0,7	0,5	0,1	0,3	0,3

DISCUSSION/ CONCLUSION

The hereby reported work focused on studying the random and systematic errors associated to treatment delivery at our department, aiming at adapting the currently implemented IGRT protocol and at revising the adopted margins in the treatment planning stage.

It was thus possible to understand that the intrafraction movements, unexpectedly, do not increase during HN treatment except for the LM direction. In fact, side-effects kick in during treatment and, although they are tackled through supportive treatment, they still may worsen and would be expected to create patient instability. The aforementioned exception might be attributed to the shape of thermoplastic masks used at our department and this question should be addressed in future work.

Future steps regarding this issue might revolve around the definition of rotational AL that, regardless of a previous guideline in the case of HN patients, should be addressed. This point is even more valid if we consider the CC direction, in which they are more severely altered.

In the case of the studied prostate group, the most increased ∑ values are observed in the AP direction. This may logically be attributed to intestinal, rectal and bladder movement. Even though all patients were carefully instructed about the rectal preparation and received information on dietary requirements during treatment, compliance with these measures is poor in a major proportion of patients. Furthermore, this might be complicated by a degree of unpredictability in the outcome of such preparations. Nevertheless, new methods to increase awareness of these issues in patients undergoing radiotherapy should be investigated, namely resorting to audiovisual material, in order to generate a clear understanding of the benefits of these simple, yet very important measures.

Moreover, the identification of systematic and random errors allow for calculation of PTV isotropic margins according to the formula devised by Van Herk et al. [20]:

$$M=2,5 \sum + 0,7\sigma.$$

For the initial phase of HN treatment, yielded values are 2,1mm, 3,5mm and 2,1mm, in the LM, CC and AP directions respectively. For the boost phase, values thus calculated are 4,0 mm, 1,6 mm e 2,7 mm in the same order. This suggests that, at our department, currently used margins, which slightly exceed these limits, ensure adequate coverage of the PTV.

In the case of prostate cancer treatment, in order to ensure PTV coverage with at least 95% of the prescribed dose, this formula generates margin values of 4,8mm, 4,3mm and 5,4mm for the initial phase in the LM, CC and AP axes respectively, whereas for the boost phase it yields 5,7mm, 6,5mm e 8,0mm, considering the same order.

Unlike the previous observation, an increase in currently used margins seems to be mandatory to ensure a safe treatment delivery. This also suggests that the random and systematic errors increase during the boost phase, which might be explained by the onset or increase of radiotherapy side-effects in this phase in the studied cohort. A possible way to tackle this problem would be treatment replanning at the boost phase, resorting to a new planning CT.

When these results are compared to the random and systematic errors reported by other authors[13-19], it is verifiable that they are in the same order of magnitude, with the sole exception of the prostate boost phase, which further stresses the importance of addressing this problem.

In conclusion, this study allowed for uncovering an eventual possibility of decreasing the PTV margins for HN cancer radiotherapy planning. It also showed that prostate margins might also be reduced during the first phase of treatment. In fact, a decrease in the irradiated volume, as defined in the ICRU 62 report [21], might account for less side-effects, with a consequent increase in patient stability and, more importantly, life-quality. These conclusions should, therefore, make way for new treatment delivery methods. Future steps should be made in order to minimize systematic and random errors associated to the boost phase in prostate patients, as to ensure more and more accuracy in radiotherapy and a consequent increment in the quality of treatment.

References:

1. Korreman S, Rasch C, McNair H, Verellen D, Oelfke U, Maingon P, Mijnheer B, Khoo V. The European Society of Therapeutic Radiology and Oncology-European Institute of Radiotherapy (ESTRO-EIR) report on 3D CT-based in-room image guidance systems: a

practical and technical review and guide. Radiother Oncol. 2010 Feb;94(2):129-44. Epub 2010 Feb 12.

2. Jaffray DA, Siewerdsen JH, Wong JW, Martinez AA. Flat-panel cone-beam computed tomography for image-guided radiation therapy. Int J Radiat Oncol Biol Phys 2002;53:1337–49.

3. Smitsmans MH, de Bois J, Sonke JJ, Betgen A, Zijp LJ, Jaffray DA, et al. Automatic prostate localization on cone-beam CT scans for high precision image-guided radiotherapy. Int J Radiat Oncol Biol Phys 2005;63:975–84.

4. Dawson LA, Jaffray DA. Advances in image-guided radiation therapy. J Clin Oncol 2007;25:938–46.

5. Purdie TG, Bissonnette JP, Franks K, Bezjak A, Payne D, Sie F, et al. Cone-beam computed tomography for on-line image guidance of lung stereotactic radiotherapy: localization, verification, and intrafraction tumor position. Int J Radiat Oncol Biol Phys 2007;68:243–52.

6. Borst GR, Sonke JJ, Betgen A, Remeijer P, van Herk M, Lebesque JV. Kilovoltage cone-beam computed tomography setup measurements for lung cancer patients; first clinical results and comparison with electronic portalimaging device. Int J Radiat Oncol Biol Phys 2007;68:555–61.

7. Perez C., Halperin E., Brady L. et al. Principles and practice of radiation oncology, fifth edition: 225

8. Jin Wang, Sen Bai, Nianyong Chen, Feng Xu, Xiaoqin Jiang, Yan Li, Qingfeng Xu, Yali Shen, Hong Zhang, Youling Gong, Renming Zhong, Qingfeng Jiang. The clinical feasibility and effect of online cone beam computer tomography-guided intensity-modulated radiotherapy for nasopharyngeal cancer. Radiother Oncol. 2009 Feb;90(2):221-7. Epub 2008 Oct 17.

9. Yan, D., Lockman, D., Martinez, A., Wong ,J., Brabbins D., Vicini,F., Liang, J., Kestin, L. Computed Tomography Guided Management of Interfractional Patient Variation Semin Radiat Oncol. 2005; 15:168-179.

10. Langen K., Jones T. Organ Motion and its Management. Int. J. Radiation Oncology Biol. Phys. 2001; 50 (1): 265–278.

11. The Royal college of Radiologists. On target: ensuring geometric accuracy in Radiotherapy. Available from: http://www.rcr.ac.uk/docs/oncology/pdf/BFCO(08)5_On_target.pdf

12. Kupelian P., Langen K., Willoughby T., Zeidan O., Meeks S. Image-Guided Radiotherapy for Localized Prostate Cancer: Treating a Moving Target. Seminars in Radiation Oncology. 2008; 18:58-66.

13. Huang E., Dong L., Chandra A., Kuban D., Rosen I., Evans A., Pollack A. Intrafraction prostate motion during IMRT for Prostate Cancer. Int. J. Radiation Oncology Biol. Phys. 2002; 53 (2): 261–268.
14. Xu F., Wang J., Bai S., Xu Q., Shen Y., Zhong R. Interfractional and intrafractional setup errors in radiotherapy for tumors analyzed by cone-beam computed tomography. Chinese Journal of Cancer. 2008; October. 27 (10): 372-376.
15. Xu F., Wang J., Bai S., Li Y., Shen Y., Zhong R., Jiang X., Xu Q. Detection of intrafractional tumour position error in radiotherapy utilizing cone beam computed tomography. Radiotherapy and Oncology. 2009. 89: 311–319.
16. Wang J., Bai S., Chen N., Xu F., Jiang X., Li Y., Xu Q., Shen Y., Zhang H., Gong Y., Zhong R., Jiang Q. The clinical feasibility and effect of online cone beam computer tomography-guided intensity-modulated radiotherapy for nasopharyngeal cancer. Radiotherapy and Oncology. 2009. 90: 221–227.
17. Nairz O, Merz F, Deutschmann H, Kopp P, Schöller H, Zehentmayr F, Wurstbauer K, Kametriser G, Sedlmayer F. A strategy for the use of image-guided radiotherapy (IGRT) on linear accelerators and its impact on treatment margins for prostate cancer patients. Strahlenther Onkol. 2008 Dec 24;184(12):663-7.
18. Sandhu A., Sethi R., Rice R., Wang J., Marcus L., Salem C.,Downs T., Kellogg J., Millard F., Pawlicki T., Mundt A. Prostate bed localization with image-guided approach using on-board imaging: Reporting acute toxicity and implications for radiation therapy planning following prostatectomy. Radiotherapy and Oncology.2008; 88: 20–25.
19. Polat B., Guenther I., Wilbert J., Goebel J., Sweeney R., Flentje M.,Guckenberger M. Intra-Fractional Uncertainties in Image-Guided Intensity-Modulated Radiotherapy (IMRT) of Prostate Cancer. Strahlenther Onkol 2008;184:668–73
20. Van Herk M. Errors and Margins in Radiotherapy. Seminars in Radiation Oncology. 2004 January; 14, (1): 52-64.
21. ICRU Report 62. International Commission on Radiation Units and Measurements. Prescribing, recording and reporting photon beam therapy. Supplement to ICRU Report 50; 1999.

GENERAL CONCLUSION:

The purpose of this study was to verify the feasibility of a previously devised IGRT protocol, as to adapt it to the observed reality at the department.

In conclusion, every prostate patient received in average 337 mGy and every HN patient received in average 13.5 mGy derived from CBCT usage during their treatments. However, if the SetD had not been corrected, there would not be a significant difference on the irradiated volume of the OAR for prostate patients, as well as a decrease in PTV coverage. In the case of HN patients, the PTV coverage would have been decreased. For all these reasons, the outcome of treatment would have been greatly modified, with a probable decrease in both toxicity outcomes and tumour control.

It was also observed that systematic errors increase during treatment for both pathologies. We should therefore rethink current strategies employed for informing patients about treatment preparation. Moreover, the data presented here supports that patients should be re-planned when they enter the boost phase.

Future research should be aimed at accounting for the dose of CBCT during the treatment planning phase. Tolerance limits, as currently applied to prostate and HN patients, should also be recalculated, This is especially important for boost margins in the case of both pathologies.